Plant Mediated Nanomaterials: An Overview on Preparation Strategies, Characterisation, and Their Potential Application in Remediation of Wastewater

Neha Kumari, Lakhan Kumar, and Navneeta Bharadvaja

Abstract Waste water containing inorganic/organic pollutants and heavy metals has become a major problem nowadays. Some heavy metals are toxic even if they are present in trace amount. So, removal through adsorption of these heavy metals is necessary as they are non-biodegradable and can easily enter in the soil and consequently harm plants and other life-forms. Nanotechnology provides a potential approach for environmental remediation as it helps in photocatalytic degradation of dyes and heavy metal adsorption from aqueous environment. Nanoparticles can be synthesized from various techniques including chemical, physical and biological. Synthesis of nanoparticles from plants is an eco-friendly, inexpensive and simple way to remediate environmental pollutants. Here, we reviewed the synthesis of nanoparticles using a wide range of plants. Plant extracts, contains a number of bioactive compounds, which serve as reducing and capping agent for the metal precursor. Plant based nanomaterials have shown ability to selectively sense the toxic hazardous heavy metals like Pb, As, Ni, Hg, Cr, Zi, Co, Fe, Mn, Pd and Se in various environmental niche. The chapter commences with the introduction to environmental degradation and discusses the phytonanoparticles synthesis approaches and their characterization. Besides this, it illustrates on role of various plant bioactive compounds in synthesis of nanomaterials. Further, it discusses role of various plant mediated nanomaterials in remediation of dyes and heavy metals. The article concludes by highlighting challenges and prospects of this emerging green technology for environmental pollution remediation.

Keywords Wastewater · Inorganic/organic pollutants · Adsorption · Photocatalytic degradation · Nanotechnology · Nanoparticles

N. Kumari · L. Kumar · N. Bharadvaja (✉)
Department of Biotechnology, Delhi Technological University, New Delhi 110042, India
e-mail: navneetab@dce.ac.in

M. P. Shah (ed.), *Modern Approaches in Waste Bioremediation*,
https://doi.org/10.1007/978-3-031-24086-7_15

1 Introduction

Phyto-nanotechnology is the emerging branch of nanomaterials synthesis from plant biomolecules that are used for a number of purposes including biomedical, microfabrication, energy storage devices, agriculture, health care, and remediation purpose as it has large surface area and high reactivity. Phyto-nanotechnology is known to be successful to reduce the environmental pollution which involves water treatment and purification of gases. Treatment of ground water is also somewhere related to inorganic and organic pollutants present in the soil. According to United Nations report, globally 0.5% of fresh water is present on earth and 80% of freshwater goes back to the ecosystem without being treated. Contaminated water and soil have become a great issue for us and the environment as well. Water can be contaminated by the presence of different chemicals and heavy metals like lead, arsenic, nickel, mercury, chromium, zinc, cobalt, and selenium. They are present in trace amount but still are highly toxic. Metallic elements are considered to be toxic due to its high density, specific gravity and atomic weight. There are 50 heavy metal presents out of which 17 are highly toxic and. normally, most of the heavy metals are found on the earth crust but due to excessive industrialization, deforestation and various other human activities these metals transfer to ground water (Chowdhury et al. 2016). Not all the heavy metals are hazardous, some are essential to humans like cobalt, copper, zinc and mercury but they can be harmful if present in excessive amount. Toxicity of a metal depends upon its dosage, chemical reaction and means of exposure. Sources of heavy metals like mercury, cadmium, arsenic, lead include coal mining, contact with acid rain, TDS refining procedure of other metals, manufacturing of chemicals and corrosion of pipes (Rosenberg 2015). Exposure of contaminated water for drinking purpose can affect human health in many ways. It can lead to several types of cancer, organ damage, neurotoxicity, nephrotoxicity, malfunction of kidney, lungs, liver, circulatory system, learning difficulty, rheumatoid arthritis and even death in extreme cases (Lellis et al. 2019). Also, in agriculture, the toxic heavy metal present in the soil can be taken up by plants leading to ROS strengthening, crops damage and adverse effect on human and animal health.

On the other hand, dyes are known to be carcinogenic and pollute water bodies. Exposure of dye in water bodies result in reduction in availability of light to the life forms living under water which leads to the reduction in the rate of photosynthesis, affecting the growth of the plant. 15–50% of azo dye is found in water bodies because it does not bind to fabric. This wastewater incorporated with dye when used in irrigation affects the soil microbial communities, enzyme activity and growth of plant. Azo dyes are chemically stable, non-biodegradable, durable coloured compounds that are carcinogenic and mutagenic in nature (Ismail et al. 2019) Congo red dye, also known as carcinogen. Benzedrine exhibit optimal, thermal and physiochemical stability which contributes to their non-biodegradable nature (Rai et al. 2014). Triphenylmethane dye used in manufacturing process such as textile dyeing, food, and cosmetics etc., causes reproductive diseases in rabbit and marine animals. O-phenylenediamine used a substrate in dyeing composition acts as a xenobiotic and

recalcitrant. It causes breathing problem, ingestion and eye irritation in humans. Brilliant Cresyl Blue is used in scientific labs and industries. Rhodamine 6 G is a fluorescent dye widely used for staining purpose but has toxic effects on microorganisms and humans. Rhodamine B dye is a water soluble red dye that causes eye and skin diseases (Glossman-Mitnik 2013). Methyl blue is a type of cationic dye extensively used in dyeing paper, clothes leather etc. Jaundice, cyanosis, high blood pressure, vomiting are some of the common diseases associated with soluble methyl blue dye (Kushwaha et al. 2014). There are many other water soluble dyes like malachite green dye, crystal violet dye, and phenol red dye that reduce the transparency of water, affect photosynthesis of aquatic ecosystem and are hazardous to humans.

Recent studies show that nanoparticles successfully remediate organic, inorganic pollutants, and heavy metals from the aqueous solution. There are several methods to synthesize nanoparticles, but biogenic synthesis of nanoparticles is chosen over other chemical and physical methods since they are simple, eco-friendly, cost effective and clean. Biological synthesis can be done from various sources like bacteria, fungi, algae and plants. In this chapter, we are focusing on phytonanotechnology which utilise plant extracts which act as reducing and capping agent in the synthesis of nanoparticles and provide stability. Generally, the plant extract is prepared as a stock and certain amount of metal precursors are allowed to react with plant extract under optimized reaction conditions. After a particular time, visual observation like colour change indicates the formation of nanoparticles without the use of any toxic, expensive chemical or the formation of any harmful by product. Metals and oxides of metals act as adsorbents following the adsorption isotherm, adsorption thermodynamics and adsorption kinetic modelling (Guerra et al. 2018). The Nano Zero Valent Iron particle is best for the reduction process as it makes use of phyto-compounds present in the plant extract. Zero valent form of iron is efficient in adsorption of hexavalent chromium (Madhavi et al. 2013a). Similarly zero valent form of silver nanoparticles removes cadmium from aqueous solution (Al-Qahtani 2017). To keep the particle stable and prevent its aggregation certain stabilizing agents are used like carboxyl methyl cellulose, sodium borohydride etc. Maghemite nanoparticles is effective against lead and cadmium from water instead of electro exploding wire techniques (Yadav and Fulekar 2018a). The chapter aims to cover several aspects of nanomaterials synthesis, their characterization and potential application in environmental remediation.

2 Synthesis of Nanoparticles

Nanoparticles are generally produced by top down and bottom-up approaches that require heavy machines, chemicals and a very high maintenance cost. So, instead of using these physical and chemical methods, biological method which is less time consuming, non-toxic and economically suitable can be preferred. The biological method involves microorganism assisted biogenesis using yeast, fungi, bacteria and algae, bio template and plant extract assisted biogenesis. In this chapter, we focused

on studying various approaches of synthesis of nanoparticles using plant extracts (Fig. 1). The biomolecules present in the plant extracts act as reducing and capping agents which help in bio-reduction of metal ions under optimized conditions. Silver nanoparticles formed from the *Gardenia jasminoides* extract help in reduction of silver ions to zero oxidation state without using any toxic chemical to form silver nanoparticles (Lü et al. 2014). Hence, bio-compounds like polyphenol, flavonoid, alkaloids, proteins, enzymes and co-enzymes help in reduction to form nanoparticles whose size depends upon the phytochemicals compounds present in the plant extract. Synthesis of metal nanoparticles with different plant extract is given in Table 1.

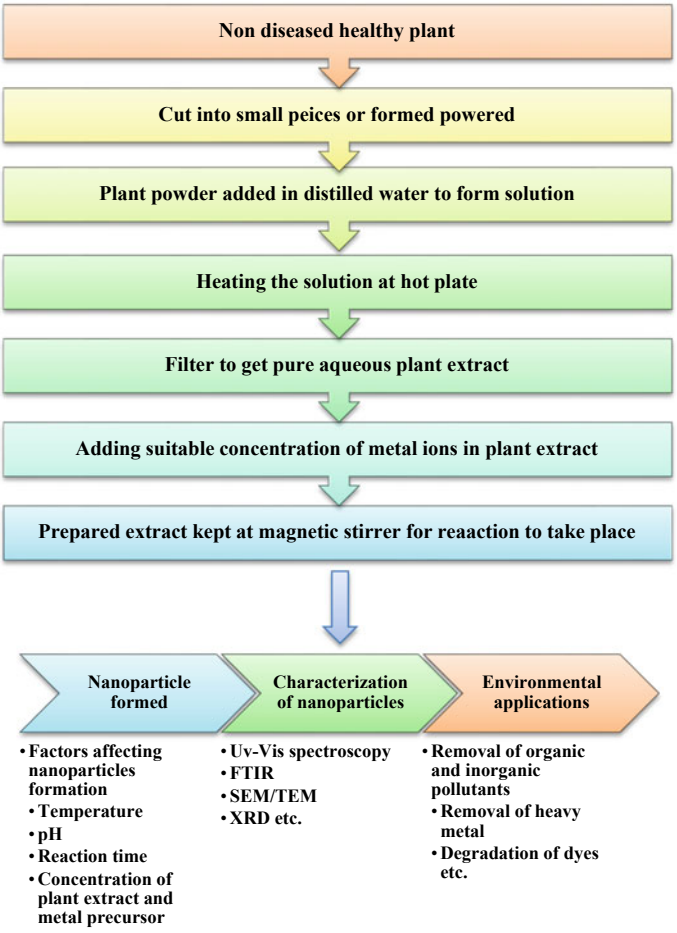

Fig. 1 Schematic representation of plant mediated synthesis of nanoparticles, their characterisation, and applications

Table 1 Nanoparticle synthesis from various plants, their characterization, and potential applications

Metal precursor	Plant	Characterization techniques					Observation		Applications	References
		UV–vis	FT-IR	SEM	TEM	EDX	Initial	Final		
Copper nanoparticle Copper sulphate pentahydrate	*Piper Retrofractum Vahl*	234–255 nm	550–570 cm	Spherical shape high Cu content-70.3%	2–10 nm	Crystallinity phase −26.4%	Yellow	Greenish black	Inhibit *E.coli* and *Staphylococcus aureus*	Amaliyah et al. 2020)
Copper nanoparticle Copper sulphate pentahydrate	*Cedrus deodara*	205 nm	607 cm	Agglomerated and form large particle	Spherical	No impurities	Greenish	Dark brown	Inhibit against pathogenic strains	Ramzan et al. (2021)
Copper nanoparticle Copper acetate monohydrate	*Punica granatum peel* extrac	–	Broad spectrum at 3400 for OH present at surfaces of CuO	Spherical shape, diameter = 12.5 mm	–	**XRD**-crystalline size = 35.80 nm monoclinic phase	Blue	Brown	Antibacterial activity against *E.coli*	Siddiqui et al. (2020)
Copper nanoparticle Copper sulphate pentahydrate (5 mM)	*Celastrus paniculatus* leaf extract	269 nm		Spherical diameter = 5 nm	2–10 nm	**DLS-** zeta potential = −22.2 mV Zeta deviation = 3.61 mV EDS-purity (79.87%)	Yellow	Green	Antifungal property Degradation efficiency on organic dye	Mali et al. (2020)
Copper nanoparticle Copper sulphate pentahydrate	*Neem* flower extract	550–560 nm		Tightly packed nanocrystal	Spherical (5 nm)	–	Light blue = light green	Dark yellow = brown ppt	**Antibacterial study** Max. efficiency against *Proteus mirabilis* = 40 mg/ml	Gopalakrishnan and Muniraj (2021)
Copper nanoparticle Copper sulphate pentahydrate	Red extract cabbage (*Brassica oleracea var. capitata f. rubra* extract)	255 nm	3100–3600 cm Band energy gap = 2.75 eV	Spherical	Particle size = 77.5 nm	**XRD-**crystalline nature, Fcc structure, crystalline size = 78 nm	–	White ppt	Antibacterial agent against *E.coli* and *S. aureus*	Fernandez and Rajagopal (2020)
Copper nanoparticle Copper sulphate pentahydrate	Seedless dates	576 nm	624.57 cm	–	Spherical	**XRD** **DLS** **Particle size distribution** = mean diameter 78 nm **Zeta potential** = +41 mV	Pale yellow	Red brown color	More feasible than chemical method	Mohamed (2020)
Copper nanoparticle Copper chloride	*Tinospora cardifolia*	248 nm	3329 cm − OH stretching 1620-C=O stretching 1395-OH bending 1319-C-O bending 1049- C-O–H stretching	Spherical	**XRD-** crystalline phase -metallic copper and copper oxide	**PSD** = 63.5 nm **Polydispersity index** = 0.26 **Zeta potential** = −33.98 mV **AFM** = 178 nm height	Sky blue	Dark green	Antimicrobial activity Efficacy of coated cotton against gram-positive is 65% & gram-negative is 50.5%	Sharma et al. (2019)

(continued)

Table 1 (continued)

Metal precursor	Plant	Characterization techniques					Observation		Applications	References
		UV–vis	FT-IR	SEM	TEM	EDX	Initial	Final		
Zinc oxide nanoparticle Zinc nitrate hexahydrate	*Cassia fistula* plant extract	370 nm	Photolytic degradation-(batch reactor) = 5 ppm dye conc. Gives 90% degradation; ph-2 & 4 96.26% & 98.71% Photodegradation efficiency Antioxidant (DPPH) Ic50 = 54 Mg/ml	Hexagonal wurtzite structure	5–15 nm	XRD- 100,002,101 plane—increases purity of particles	–	–	Exhibit Antioxidant, Bactericidal property and catalytic property against methyl blue	Suresh et al. (2015)
Silver nanoparticle Silver nitrate	*Morinda tinctoria* Leaf extract	420 nm	3296 cm—carboxylic group 3436–3220 cm—O–H stretching, H bonded phenol and alcohol group 1634 cm—N–H bending primary amines 1672 cm—C = O stretching	Spherical rod shaped	79–96 nm	4 peaks of 2 theta 38.26 degree = (111) 44.44 = (220) 64.58 = (220) 77.67 = (311) Fcc and crystalline in nature	Pale yellow	Dark brown	Degradation of methyl blue dye	Vanaja et al. (2014)
Silver nanoparticle Silver nitrate	Neem leaf Neem bark Mango leaf Green tea Pepper seeds	420	-	Spherical	–	–	Pale yellow	Brownish yellow	Calorimetric sensing of toxic metal (Hg2+, Pb2+, Zn2+, Cr 3+, Cd2+, Ca2+. Cu2+, Mg2+, Ni2+, Fe2+)	Karthiga and Anthony (2013)
Silver nanoparticle Silver nitrate	*Amaranthus gangeticus Linn leaf extract*	416 nm	1635 cm—C = O stretching 3441 cm—OH & NH2	Globular shaped	11–15 nm	–	–	Brown	Antifungal and antibacterial activity inhibitory activity towards gram +ve & − ve Degrade congo red dye	Kolya et al. (2015)
Silver nanoparticle Silver nitrate	*Nigella Sativa* seed extract	426 nm	3423- 2880 cm Indicates CH, −OH, −NH, C=C acting as reducing & stabilizing/capping agent	Spherical	10.88 nm	XRD- 2 theta = 38.14 degree- (111); 44.36 degree (200); 64.71 (220) 77.40 (311)	White	Light brown	Congo Dye degradation	Chand et al. (2021)

(continued)

Table 1 (continued)

Metal precursor	Plant	Characterization techniques					Observation		Applications	References
		UV–vis	FT-IR	SEM	TEM	EDX	Initial	Final		
Silver nanoparticle Silver nitrate	*Zanthoxylum armatum* leaves	419 nm	3431 cm- N–H stretching OH hydroxyl grp 2922 cm- C-H stretching 1744 cm—carbonyl stretching 1630 cm- N–H bond 1375 & 1238 cm—N = O symmetry 1045 cm- C-N amines	Spherical shape	Diameter = 15–20 nm	**Zeta potential** = −21.2 mV Average size −36 nm **XRD** Fcc 2 theta = 38.23 degree (111); 46.45 (200); 66.65 (220); 77.55 (311) Avg crystallize size—22 nm	Colourless	Brownish	Dye degradation—safranin O Methyl red Orange and methyl blue	Jyoti and Singh (2016)
Silver nanoparticle Silver nitrate	*Viburnum opulus* fruit extract	513 nm; 415 nm (350–450 nm)	3398 cm- stretching of O–H 1733 cm- C=O stretching 2931 cm—C-H stretching 1380 cm-C-O stretching 1030 cm- C-O bending	Spherical	7–26 nm Avg size- 16 nm	**XRD-** 2 theta 38.33 degree (111); 44.56 (200); 64.62 (220); 77.44(311);82.41 (222); 32.2- organic compound in sample (Fcc) **TGA-** 35.14% bioactive compounds present at AgNP surface	Faint red	Yellowish brown	Dye degradation Brilliant blue Tartrazine Carmoisine	David and Moldovan (2020)
Silver nanoparticle Silver nitrate	*Calendula officinalis*	436 nm	2 theta – 665 cm; 3438 cm; 1635 cm- stretching vibration of carbonyl grp; 3338 cm- O–H stretching	Uniform and spherical	50–60 nm 140–150 nm	**XRD-** Fcc, crystal size = 14.37 nm	Yellow	Brown	Methyl blue and methyl orange degradation	Chandra Paul et al. (2020)
Silver nanoparticle Silver nitrate	*Dahlia pinnata* leaf extract	460 nm	1064 cm- C-N bond 3265 cm- O–H stretching 2916 cm- C-H stretching 1423 cm- C-H bending 673- stretching vibration of halo alkene 1595 cm- C-H present	Almost spherical	Diameter- 15 nm	**XRD-** Face centre cubic structure, 27.5- (220); 32.75- (122); 46.25(111); 54.65(331); 57.25(241); 76.68(311)	Colourless	Dark yellow	Rapid colorimetric detection of Hg2 +	Roy et al. (2015)
Silver nanoparticle Silver nitrate	*Panax Ginseng* root extract	404 nm	3640 cm- O–H stretching 1740- carbonyl stretching vibration of aldehyde 1640- symmetry-COO stretching 1407- asymmetry-COO stretching 1065- bending vibration of C–C-O & C–C-OH	spherical	4–20 nm	–	–	Dark brown	Detection of Hg2+	Tagad et al. (2017)

(continued)

Table 1 (continued)

Metal precursor	Plant	Characterization techniques					Observation		Applications	References
		UV–vis	FT-IR	SEM	TEM	EDX	Initial	Final		
Gold nanoparticle Gold(lll)chloride trihydrate	*Capsicum annum*	335.26 nm	3324- 3329 cm- = −OH grp 2100 cm- -CN grp 1636 cm- C = O grp	Triangular	–	**XRD-** 111, 200, 220, 311 degree Crystal size = 13.71 nm	Yellow	Dark red	Water pollution removal and Show strong antimicrobial activity at low concentration	Baran et al. (2020a)
SnO2 nanoparticle (SnCl2)	*Vitex agnus-castus* fruit extract	373.45 nm	3434.27 1633.02 1027.50 647.45 Anti-symmetric Sn–O-Sn; Sn–O symmetric	Spherical	4–13 nm Avg size = 8 nm	**XRD** 26.9 degree- (110);34- (101); 38-(200); 52-(211); 58-(002); 62.1-(310); 65.2-(301); 71.4(202)	–	Light grey	Photocatalytic degradation of organic dye RhB, under and removal of heavy metal Co+2	Ebrahimian et al. (2020)
Iron nanoparticle (FeSO4.7H2O)	*Eucalyptus globules* leaf	'graph given = above 420 nm	3346.25 cm; 1635.58; 524.68 cm (polyphenolic content present	Spherical	50–80 nm	**XRD** Peak at 2 theta 46.40 indicates zero valent iron	Brown	Black	Adsorption of Cr(VI)	Madhavi et al. (2013a)
Maghemite nanoparticle 2 M FeCl3+1 M FeSO4.7H2O	*Tridax* plant	210 nm	454 cm, 569 cm, 632 cm, attributed to Fe–O; 563 cm—gamma attributed to FeO 1443–1600 attributed to C=C/C=N bond 326, 402, 500, 706 are peaks of Maghemite	Cubic spinal structure (spherical and cuboidal shape)	9.59–15.42 nm	**XRD** 18.22, 29.3,30.02,32.08,43.14,57.48 degree with miller indices 011,210,220,310,330	–	Blackish brown ppt	Removal of heavy metal Pb and Cd	Yadav and Fulekar (2018a)
Zinc Nanoparticle Zinc acetate (0.1 M)	*Sphagneticola trilobata* (leaf, stem and root extract)	-	3144 cm-C=O stretching 1665 cm −N–H stretch 1640 cm-N–H bending in amine & amide grp	Irregular and complex	65–80 nm	**EDS-** zinc 41.4% synthesized in Nanomaterial **XRD-** 200,111,221 planes correspond to 2 theta angle Face center cubic structure	–	Yellow colour	Removal of Chromium by DPC method	Shaik et al. (2020a)
Cupric Oxide nanoparticle	*Calotropis procera*		3444 cm −OH grp; 1636 cm; 1231 cm;1084– protein latex 519; 598 cm −Cu–O band	Spherical	10–15 nm; diameter = 15.06 nm standard deviation- 5.17	**XRD** Peak on range 20 < 2 theta <80 degree Monoclinic symmetry	Green ppt	Black ppt	Removal of Cr(VI) from aqueous solution	Dubey and Sharma (2017)

(continued)

Table 1 (continued)

Metal precursor	Plant	Characterization techniques					Observation		Applications	References
		UV–vis	FT-IR	SEM	TEM	EDX	Initial	Final		
Iron based NP FeSO4.7H2O	*Eucalyptus leaf*	–	3388 cm −O–H stretching; 2932 &2840 −C-H stretching;1720—carbonyl grp; 1605& 1515 −C=C aromatic skeletal vib.;1330 −CH3 asymmetric vib.;1048- C-N stretching NP rxn with Cr(VI) & Cu(II) show band at 460 & 546 cm -Fe–O stretch	Polydispersed	20–80 nm	**EDS-** Element % of Fe = 16.3; C = 47.4 O = 36.3 **XRD** 2 theta at 44.8; 24 degree show biomolecule capped with Fe NP	–	–	Removal efficiency of Cr (VI) and Cu (II) when existed together or separated	Weng et al. (2016a)
Zero valent silver NP Silver nitrate	*Ficus Benjamina*	420 nm	3461- O–H stretching; 1632 cm—amide grp	Dendritic structure	60–105 nm	–	–	Brown	Cadmium removal from aqueous solution	Al-Qahtani (2017)
Zero valent Iron NP	*Rose damascene, Thymus vulgaris, Utrica dioica* leaf extract	–	3400 & 3430 cm for polyphenols; 1126–1190 cm for carbonyl grp; 1628 &1640 cm corresponds to C=C in alkene grp; 615–617 indicating aromatic compounds of alkanes	Non uniform exhibit differed space & void space	100 nm **BET** Surface area = 1.63(TV); 2.42(UD); 1.42 (RD)m3/g total pore vol = 4.52*10–2(TV) $2.97*10^{-2}$ (UD); $2.08*10^{-2}$ (RD)	**XRD** Perfectly index crystalline Fe	–	–	Removal of Cr(VI) from aqueous solution	Fazlzadeh et al. (2017)
Silver nanoparticle Silver nitrate	*Perilla frutescens*	469 nm	615 & 627- C-H group; 1048 & 1124—stretching vibration; 1381 &1374 -C-N stretching vibrations; 1608 & 1601- secondary amide groups	Spherical, rhombic, triangular and rod shaped	25.71 nm	**Zeta potential-** −23.33 mV FCC cubic	Yellow	Brown	Exhibits antioxidant, anticancer and antibacterial properties	Reddy et al. (2021)
Copper nanoparticle $Cu(OAc)_2$	*Stachys lavanaulifolia*	400 nm	3100–3385-hydroxyl group; 2922, 1618, 1398 represent saturated hydrocarbon; C=C and C=O—aromatic stretching frequency; 3400- O–H stretching; 1473-bonding vibration of sp^2 bond 1627- carbonyl stretching	Monodispersed	20–35 nm	**XRD** 2 theta = 32.59, 35.61, 38.78, 48.82, 53.24, 58.37, 61.60, 66.31, 68.15, 72.46, 75.30 assigned to (110), (−111), (111), (−202), (020), (202), (−113), (220), (311), and (-222) planes	Pale yellow	Dark brown	Represents catalysed C-heteroatom coupling reaction	Veisi et al. (2021)

(continued)

Table 1 (continued)

Metal precursor	Plant	Characterization techniques					Observation		Applications	References
		UV–vis	FT-IR	SEM	TEM	EDX	Initial	Final		
Iron based nanoparticle $FeSO_4.7H_2O$	Green tea extract	–	1611- C = C stretching vibrations; 1362- C-N bond; 1039- C–O–C bonding	–	50–80 nm	**GC–MS** Phenol, 1,1-biphenyl, 2-ethyl, 1,2,3- benzenetriol, caffeine and bis (2-ethylnexyl) phthalate involve in FeNP synthesis as reducing and capping agent			Removal of hexavalent chromium	Hao et al. (2021)
Nickel oxide nanoparticle $Ni(NO_3)_2.6H_2O$	*Abutilon indicum* leaf extract	200–385 nm	3410 (O–H); 2990 (C-H); 1702 (C = O) 1650 (amine I and amide II); 1259 (O–H) 1140 (C-O)	Agglomerated form	452.49 nm	**XRD** Highly crystalline attributed to (111), (200), (220), (311), (222) plane with diffraction angle 37.5, 43.26, 63.11, 75.46, 49.46 degree respectively	Yellow	Green	Exhibit anticancer, antioxidant, and antibacterial property	Khan et al. (2021)
Zinc oxide- based nanoparticle $Zn(NO_3)_2.7H_2O$	*Saponaria officinalis* extract	380 nm	-	Agglomerated form	100–200 nm diameter	**XRD** Hexagonal wurtzite phase attributed to (100), (002), (101), (102), (210), (103), (200), (212), (201) planes		Dark brown	Dye degradation efficiency of methyl blue and show antibacterial activity	Tănase et al. (2021)
Silver nanoparticle Silver nitrate	Plant gum of- *Araucaria heterophylla* *Azadirachta indica* *Prosopis chilensis* (bark of tree)	–	–	Spherical	30 nm DLS = 50 nm 35 nm; DLS = 50 nm 50 nm DLS Diameter = 75 nm	**Zeta potential (EDX)** −20.87 mV −23.65 mV 16.41 mV			(1) Effective against gram positive and gram-negative bacteria (2) not much effective against cell lines, but still exhibit anticancer anti-cancer activity against human breast cancer cell line MCF 7 at higher concentration (3) Chromium removal efficacy was not efficient	Samrot et al. (2019)

3 Role of Phytocompounds in Nanoparticles Synthesis

Phytocompounds play a major role in the formation of nanoparticles. Due to extensive study on phytochemicals analysis, our understanding has increased about them. It has facilitated in identification of particular biochemical compound present in the plant which acts as a reducing, capping and stabilising agent in nanoparticles synthesis. The phytochemicals analysis, if carried out by performing phytochemicals tests can give the exact phyto component participating in reduction, which can be further determined by FTIR (Fourier Transform Infrared Spectroscopy) analysis. FTIR studies reveal that amino acids help in reduction of metal ions. For example, alpha amino acids reduces silver ion (Tan et al. 2010). Flavonoids are secondary metabolites produced by plants that have the ability to transform enol-form to keto form by releasing one hydrogen atom. Functional group of phenolic acids comprises the phenolic ring which is responsible for chelating metal and carboxylic acid. In synthesis of silver nanoparticle, using plant extracts of three plants namely *Schinus molle, Equisetum giganteum*, and *Ilex paraguariensis*, removal of electrons occur so that Gallic acid is oxidised to quinine (Barberia-Roque et al. 2019). Phytocompounds polyols and polysaccharides actively present in *Cinnamomum verum* help in reducing Ag + ion in silver nanoparticle synthesis (Sathishkumar et al. 2009). Its functional group containing carbohydrate and hydroxyl group is known to be soluble in water while methyl and isopentyl are lipophilic in nature. It also has potential to donate hydrogen atom, thus helping in reduction process. Flavonoids are divided into major subclasses which included chalcones, flavones, flavanols, isoflavones and anthocyanidin. Quercetin, which comes under the class of flavanol, chelates metal ion at three different positions namely the catechol group, carbonyl group and hydroxyl group. Quercetin and plant pigmentation helps in bioreduction of silver nanoparticle synthesized from *Acalypha indica* leaf extract (Krishnaraj et al. 2010). Flavonoids have potential to tolerate heavy metals like cadmium and zinc in *Arabidopsis thaliana.* Terpenoids are the derivative of essential oil and have diverse structure containing 5 carbon isoprene units. They show strong antioxidant activity. They also help in bio-reduction by deprotonating the OH^- group to form conjugate base structure and preventing it from further oxidation. Terpenes, which are converted into terpenoids upon oxidation, help in metal reduction. This active redox reaction leads to the formation of nanoparticles. *Lantana camara* leaf extract contains terpenoids as their main reducing and capping agent in the synthesis of silver nanoparticles (Ajitha et al. 2015). Excessive thermal heating can inactivate essential phytocompounds. Monosaccharide sugar like glucose and fructose also take part in formation of metallic nanoparticles through the conversion of ketone to aldehydes. Disaccharides and polysaccharides form an open chain with the help of monosaccharides up to 7–8 units and provide the metal ion to aldehydes group and facilitate reduction process.

4 Characterization of Nanoparticles

To detect the reduction of metal precursor, the optical absorbance of synthesised nanoparticles is performed by a UV–Vis spectrophotometer. The spectra are recorded within the range of 200–700 nm. UV–Vis spectrophotometer is used to determine the concentration of different molecules present in a solution utilising the characteristics wavelength of the molecule at which it maximally absorbs the light. After the plant extract and metal precursor are mixed, a change in colour of the solution is observed as the time progress. One concern is there that with time aggregation of nanoparticles proceeds, which ultimately alter the peak of absorbance. At particular wavelength of localized surface plasmon resonance, we get different maximum absorbance of nanoparticles as compared to literature values of those particular metal precursors. A study reported that the gold nanoparticles synthesized from *Garcinia mangostana* fruit peels turned purple instead of traditional yellow (Xin Lee et al. 2016). Maximum absorbance of silver and gold nanoparticles synthesized from *Rumex roseus* leaf extract was recorded at 429 nm and 549 nm respectively by UV–Vis spectrophotometer (Chelly et al. 2021). SEM/TEM is used to determine the morphology of the synthesized nanoparticles. In TEM analysis, once electron hit the sample it gets absorbed, and gives much higher resolution than light microscopy whereas in SEM analysis of nanoparticles, the electron scans for different region of sample. In some regions, more scattered electrons are present due to which the absorbed atom is less and in other region less scattered electron found give a clear indication of more absorbed atom. This scattering of electron in different region results in more contrasting three- dimensional image as obtained from SEM micrograph. SEM/TEM studies are done to observe the shape and size of the synthesised nanomaterials. *Garcinia magostana* mediated magnetite nanoparticles are of 13.42 nm and displayed diffraction rings of Fe_3O_4 phase (Yusefi et al. 2021). FTIR spectra determine the functional group present in the plant extract which are held responsible for the synthesis of nanoparticles. The principle behind FTIR tell us that the bond between two atoms or molecules are not fixed and are involved in different types of motions called bond vibrations. Every compound has its signature vibration and stretching between the bonds by which the functional group can be determined. For example, formaldehyde has carbonyl carbon attached with oxygen where stretching and wagging goes on simultaneously. Therefore, absorbance determines the type of functional group present in the sample. The peaks in the spectrum show the bending and stretching vibrations of the biomolecules. Zinc oxide nanoparticles synthesized from *Cayratia pedata* leaf extract exhibit zinc bonding at 400 cm^{-1} and oxygen bonding at 600 cm^{-1} (Jayachandran and Nair 2021). Crystal structure of nanomaterials are analysed by XRD. We use X-ray crystallography because X-ray has shorter wavelength. Its working involves projecting a high energy electron beam falls on a rotating target that throws out the X-ray generated, which are then measured by a detector containing photomultiplier tube of X-ray diffractometer. The position of the peaks is determined by the planes which diffract coherently at an angle where Bragg's law holds good.

5 Different Types of Plant Mediated Nanoparticles Helping in Dye Degradation and Heavy Metal Removal from Aqueous Solution

Chemical compounds which are released from industries, households, oil pollution, acid rain, sewage and agriculture waste makes remediation process of water more complicated and difficult. There are many techniques available for purification of water but the nanotechnological approach has been termed as potential method due to the small size and high reactivity of nanoparticles. Several types of plant-based nanomaterials have been explored for remediation of environmental pollutants as illustrated in Fig. 2.

5.1 Nanoscale Zero Valent Iron (nZVI) Nanoparticle

Nanoscale zero valent iron (nZVI) is preferred because it can be separated easily under the influence of external magnetic field. nZVI cannot remove contaminants on its own because of high probability of aggregation which can easily alter the surface chemistry to make it unreactive (Pasinszki and Krebsz 2020). To prevent these problems, nZVI nanoparticles come into use without damaging the active catalytic sites of nZVI. Sodium borohydride is used for stabilizing these nanoparticles as it increases surface reduction and prevents oxidation. Polyvinyl-pyrrolidone (PVP), polyethylene glycol (PEG), and carboxymethyl cellulose (CMC) used in coating of nZVI increase the stability by catalytic reduction of ketones to alcohol (Parimala

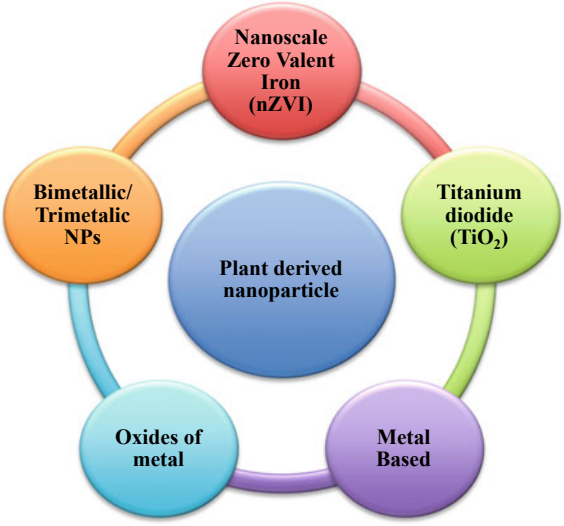

Fig. 2 Types of plant derived nanoparticles

and Santhanalakshmi 2014). Fenton's reagent is also used in remediating wastewater along with nZVI nanoparticle as it produces hydroxyl radicle at low pH with higher concentration of H_2O_2 and Fe^{2+}. Reduction of oxygen by nZVI and subsequent formation of hydrogen peroxide leads to hydroxyl radical formation and an oxidized organic compound (Babuponnusami and Muthukumar 2014). Nanoscale zero valent iron nanoparticle synthesis from green tea extract using bentonite for stabilization successfully degraded 96.2% RB 238 dye within 60 min followed by Fenton like oxidation (Hassan et al. 2020). Catalysis of dye resulted in the formation of hydrogen peroxide in which the OH radicle and dye degraded to form carbon dioxide and water molecule. Nanoscale zero valent iron used along with magnetite nanoparticle followed Fenton's reaction to remediate wastewater by degrading chlorinated compound like 2, 4-Dichlorophenoxyacetic Acid at pH 3–6.5 within 90 min (Nanoparticles 2020).

5.2 Titanium Dioxide (TiO_2) Nanoparticle

Titanium dioxide obtained from the three different minerals namely anatase, brookite and rutile. Anatase grade of TiO_2 exhibits similar properties as of rutile but brookite form is very rarely formed and is highly unstable. TiO_2 nanoparticle synthesized from Cinnamon powder are of spherical anatase phase and shows enhanced photocatalytic property for solar cells with band gap of 3.2 eV which is determined by UV–Vis spectroscopy (Nabi et al. 2020a). Titanium dioxide is a potent photocatalyst which gets activated by UV light such as sunlight for photocatalytic reaction to take place. Titania exhibits unique physical properties due to which TiO_2 is insoluble in water and show white colouration or precipitate, that's why it is extensively used as food additive. Chemical and physical methods have several limitations like small scale production, not environment friendly, maintenance of temperature and pressure leads to high cost, use of surfactants result in toxicity and complexity. TiO_2 nanoparticles can be successfully synthesized from biological methods like *Aloe vera* extract, *Annona squamosa* peel extract, and *Jatropha curcas* leaf extract, *Nycetanthes Arbor-Tristis* leaf extract, *Psidium guajava* and various other plant extracts given in Table 2.

TiO_2 is another way to generate hydroxyl radical which oxidizes contaminants present in water under the influence of light. Under the exposure of UV light, the band energy gap of TiO_2 is 3–3.5 eV. The transfer of negative charged electron from valence band to conduction band exhibited by the forming positive charged holes. The photogenerated positive charge carriers (holes) from valence band diffuse to photocatalyst surface and react with water molecule to form free radical which is further oxidizes (Nakata and Fujishima 2012). The negatively charged electron from conduction band helps to promote reduction followed by reacting with atmospheric air to produce non-hazardous compound like water molecule, carbon dioxide etc. To enhance the photocatalytic efficiency, TiO_2 is trapped within nanoparticles without damaging the active sites followed by surface modification via doping with carbon, nitrogen and metal (Zahra et al. 2020).

Table 2 Types of phyto-nanoparticles and their application in treatment of wastewater

Type of nanoparticles	Plant source	Absorption capacity/percentage degradation	Applications	References
nZVI	*Rosa damascene (RD)* *Thymus vulgaris (TV)* *Utrica dioica (UT)* leaf extract	94.87% 83.45% 86.8%	Removal of Cr(VI)from aqueous solution	Fazlzadeh et al. (2017)
Kaolin-supported nZVI	*Ruellia tuberosa*	99.8%	Degradation of reactive black 5 azo dye	Khunjan and Kasikamphaiboon (2021)
nZVI	*Spinacia oleracea*	COD- 73.82% BOD- 60.31%	Removal of chemical and biological oxygen demand from municipal waste water	Turakhia et al. 2018)
nZVI	*Cupressus sempervirens*	95.4%	Decolourization efficiency of methyl orange	Ebrahiminezhad et al. 2018)
nZVI	Oak Mulberry Cherry Leaf extract	–	Removal of As(III) and Cr(VI) from aqueous solution	Poguberović et al. (2016)
nZVI	*Mentha piperita*	PO_4^{3} −85.01% NH_3 −99.51% NO_3 −86.33% Pb^{2+} −83.4% Cl −79.33%	Removal of agricultural contaminants like phosphate, ammonia, nitrate, lead, and chloride from aqueous solution	Shad et al. (2020)
nZVI	*Shorea robusta* leaf extract	96%	Degradation of congo red dye from aqueous solution	Jha and Chakraborty (2020)
nZVI	Grape seed extract + Fe^{3+}	82.8–96.1%	Removal of Cr(VI) from aqueous solution	Guo et al. (2020)

(continued)

Table 2 (continued)

Type of nanoparticles	Plant source	Absorption capacity/percentage degradation	Applications	References
nZVI	*Ficus Benjamina* leaf extract	75.5–85%	Cadmium removal from aqueous solution	Al-Qahtani (2017)
TiO_2 Au-TiO_2	*Azadiracta indica*	–	Degrade methyl red dye	Sankar et al. (2015)
	Cinnamomum tamala leaves	64%	Degradation of methyl orange	Naik et al. (2013)
	Jatropha curcas leaf	82.26% 76.48%	Removal of chemical oxygen demand(COD) Removal of Cr from tannery wastewater	Goutam et al. (2018)
	Piper betel (PS) *Ocimum tenuiflorum* (OT) *Moringa oleifera* (MO) *Cariandrum sativum* (CS)	MO degrades faster among all within 30 min	Degradation of malachite green dye	Pushpamalini et al. (2020)
	Lemon peel extract	70%	Degradation of rhodamine B dye	Nabi et al. (2020b)
	Syzygium cumini leaf extract	75.5% 82.53%	Photocatalytic removal of chemical oxygen demand (COD) Removal of lead (Pb)	Sethy et al. (2020)
TiO_2	*Caltropis gigantea* leaf extract	96.7%	Catalytic degradation of metformin by solar photocatalysis	Prashanth et al. 2021)
Metal -FeNP	Green tea extract	81% 31%	Removal of methyl chlorobenzene (MCB) from wastewater Removal of chemical oxygen demand(COD)	Kuang et al. (2013)

(continued)

Table 2 (continued)

Type of nanoparticles	Plant source	Absorption capacity/percentage degradation	Applications	References
FeNP	*Eucalyptus leaf* extract	N-71.7% COD-84.5%	Removal of total nitrogen and COD from wastewater	Wang et al. (2014)
Nickel NP	*Camellia sinensis* leaf extract	94.5%	Degradation of CV dye	Bibi et al. (2017)
AgNP	*Morinda tinctoria* leaf extract	95.3%	Degradation of methyl blue dye	Vanaja et al. (2014)
FeNP	*Camellia sinensis leaf extract* *Vitis vinifera extract*	RR-52% RY-64% RB-78% RRB-76% RR-49% RY-61% RB-71% RRB-68%	Degradation of Reactive Red 195 (RR), Reactive Yellow 145 (RY), Reactive Blue (RB) and Reactive Black 5 dyes	Raman et al. (2021)
AgNP	*Nigella sativa* seed extract	98.5%	Decolouration of Congo red dye	Chand et al. (2021)
AgNP	*Zanthoxylum armatum* leaves	SO-1.02 $\times$ 10^{-3} MR-1.03 $\times$ 10^{-3} MO-1.86 $\times$ 10^{-3} MB-1.44 $\times$ 10^{-3}	Dye Degradation of safranin O (SO), Methyl red (MR), Methyl orange (MO), Methyl blue(MB)	Jyoti and Singh (2016)
AgNP	*Calendula officinalis*	MB- 27.12% MO-69.79%	Degrade methyl blue (MB) and methyl orange(MO) dye in aqueous solution	Chandra Paul et al. (2020)
AuNP	*Capsicum annum*	Pb-63.46% Cd-60.20% Cu-51.50% Fe-68.20% Ni- 42.18% Co- 23.47% Mn-21.62% Zn-35.37% Pb-75.75%	Removal of contaminant present in water including Pb, Cd, Cu, Fe, Ni, Co, Mn and Zn	Baran et al. (2020a)

(continued)

Table 2 (continued)

Type of nanoparticles	Plant source	Absorption capacity/percentage degradation	Applications	References
SnO_2 NP	*Vitex agnus castus* fruit extract	RhB- 91.7% Co^{+2}–93.6%	Photocatalytic degradation of Rhodamine B dye and removal of heavy metal Co^{+2}	Ebrahimian et al. (2020)
FeNP	Green tea extract	19.9 mg/g	Removal of As (V) at 298 K	Wu et al. (2021)
Oxide of metal—iron	Pomegranate seed extract	95.08%	Degradation of reactive blue 4 dye from aqueous solution	Bibi et al. (2019)
iron	*Cynometra ramiflora* fruit extract	94%-91%	Degradation of methylene blue dye under sunlight irradiation	Bishnoi et al. (2018)
iron	*Piper betle* leaves	MG-93% MO-73.29%	Degradation of malachite green (MG) and methyl orange (MO) dyes	Badmapriya and Asharani (2016)
Copper	*Carica papaya* leaf extract	–	Degradation of Coomassie brilliant bye R-250 dye	Sankar et al. (2014)
Copper	*Pridium guajava* leaf extract	NB- 93% RY160-81%	Degradation of Nile blue (NB) dye and reactive yellow (RY160) dye	Singh et al. (2019)
Alpha- manganese oxide	*Ficus Retusa*	MO- 116.1 mg/g MR- 74.02 mg/g	Determining adsorption efficiency of azo dye like methyl red and methyl orange	Srivastava and Choubey (2021)
Zinc	*Carissa edulis* extract	97%	Degradation of Congo red dye	Fowsiya et al. (2016)
Zinc	*Trianthema Portulaca* strum's extract	91%	Show antimicrobial activity against Staphylococcus aureus and E.coli, Antifungal activity against *Aspergillus niger* and *Aspergillus flavus* and degradation of Synozol Navy blue-KBF textile dye under solar irradiation	Khan et al. (2019)

(continued)

Table 2 (continued)

Type of nanoparticles	Plant source	Absorption capacity/percentage degradation	Applications	References
Zinc	*Calliandra haematocephala* leaf extract	88%	Catalytic degradation of methylene blue dye under solar radiation	Vinayagam et al. (2020)
Zinc	*Saponaria officinalis*	42%	Degradation of methyl blue and exhibit antibacterial property	Sharma et al. (2019)
Bimetallic—Fe/Pd NP	Grape leaf aqueous extract	98%	Removal of orange (II) dye	Luo et al. (2016b)
nZVI/Ni	Green tea extract	100%	Removal of Cr(VI) for groundwater	Zhu et al. (2018)
Ni/Fe NP	*Punica granatum* peel extract	76–78%- groundwater 68–72%- lake water 92–94%- DW	Removal of tetracycline from ground water, lake water and deionized distilled water	Ravikumar et al. (2019)
nZVI-Cu NP bentonite supported nZVI-Cu NP	Pomegranate rind extract	72% 95%	Removal of antibiotic tetracycline from natural water	Gopal et al. (2020)
Ag/AgCl NP	*Azadirachta indica*	92.5%	Degradation of methyl blue dye from aqueous solution and exhibit antibacterial property	Panchal et al. (2021)
Mn:CeO_2	*Cassia angustifolia* Seed extract	–	Photo degradation of malachite green dye	Antony and Yadav (2021)
$NiFe_2O_4$ NP	*Juglans regia*	85%	Photocatalytic degradation of congo red dye and ciprofloxacin from water	Taj et al. (2021)

5.3 Metal and Metal Oxide Nanoparticle

Metals and oxides of metal nanoparticles are governed by physical and chemical properties of metals which play a major role in providing stability. Also, catalytic property enhances the degradation of contaminants like toxic metals, organochlorinated pesticides, polychlorinated biphenyl (PCB) (Nguyen et al. 2018). Metal oxide nanoparticles are very specific to size, shape as well as nanostructure. They have high density which results in small size of nanoparticles. So much of concern with the size is related to reactivity, magnetic and electric property of nanomaterials. Rather than remediating wastewater, iron oxide and magnetite are also considered as a potential approach in MRI and MSD. Similarly, silicon dioxide, manganese oxide, copper oxide, zirconium oxide, acts as catalysts in oxidation process and also possess electrolytic property. CeO_2 nanoparticle synthesised from *Oleo Europaea*, *Rubia cordifolia* leaf show various catalytic properties, used in medical sciences and optical sensor technology (Nadeem et al. 2020). Iron oxide nanoparticle conflicts our interest, used in removal of contaminants from water. iron oxide nanoparticle potentially removes lead, cadmium and chromium from aqueous solution (Ehrampoush et al. 2015). Bio-compounds such as coumarin and olefins facilitates reduction of metal ion by donating electron followed by hydroxyl and methyl group containing compound. polyphenolic compounds chelate the metal ion therefore nanoparticle can be reused up to five cycles without losing stability (Groiss et al. 2017). Several examples of metallic nanoparticles and metal oxide nanoparticles are given in Table 2.

5.4 Bimetallic/Trimetallic Nanoparticle

Combination of metals by optimizing their energies and reaction conditions refers to bimetallic or trimetallic nanoparticles based upon the number of metals participating in the formation and enhance their remediation strategy. They can be used as multipurpose tool. Bimetallic increases the efficacy of reduction of metal by altering the individual component, or geometrical structure to achieve better functionality and application. *Phoenix dactylifera* synthesised bimetallic copper-silver nanoparticle exhibit catalytic property to degrade methyl blue from aqueous solution and antibacterial activity against *Bacillus subtilis* and *Escherichia coli* (Al-Haddad et al. 2020). Some monometallic nanoparticle aggregates easily and loss their reactivity therefore addition of catalytic metal is preferred which result in formation of bimetallic nanoparticle in order to increases the reactivity, catalytic selectivity and great efficiency useful in multiple applications like exhibiting antimicrobial property, anticancer property and potent nano catalyst. Green synthesis of Au–Ag bimetallic nanoparticle by using *Pulicaria undulata* extract shows catalytic activity in reduction of 4-nitrophenol to 4-aminophenol under the influence of sodium borohydride (Khan et al. 2020). Silver nanoparticle which exhibits excellent antibacterial property used in pharmaceutical sector and antimicrobial property used in cosmetics, biosensor,

food processing etc,. On the other hand, gold nanoparticle used in medical field like cancer therapy. The idea is to combine the dual nature of silver and gold nanoparticle to improve the application and efficiency in bimetallic nanoparticle. Fe/Pd nanoparticle synthesis from aqueous extract of grape leaf in order to determine the reactivity of bimetallic nanoparticle in comparison with monometallic iron nanoparticle (Luo et al. 2016a).

Green synthesis of Au/Pt/Ag trimetallic nanoparticle using *Lamis albi flos* extract for determination of antimicrobial activity (Dlugaszewska and Dobrucka 2019). *Vitex angus-castus* synthesized Au-ZnO-Ag trimetallic nanoparticle has ability to degrade methylene blue dye within 36 min as well as 97% degradation of crystal violet dye (Dobrucka 2019). Nanomaterial along with nanoparticles is more specific in treatment of water as it increases the degradation speed and reactivity, preventing any kind of by product formation. Nanomaterials when reacts with pollutants (inorganic/organic) or heavy metals, result in photocatalytic reaction, chemical reaction, absorption and adsorption. Au–Ag-Sr nanoparticle synthesize from root extract of three different plants namely *Coriandrum sativum, Aloe indica* and *Plectranthus amboinics* by using gold chloride, silver nitrate and strontium chloride as a metal precursor (Binod et al. 2018). Trimetallic Fe-Ag-Pt synthesize from *Platycodon grandiflorum* shows excellent catalytic efficiency in reducing 4- nitroaniline to p-phenylenediamine within 25 min and complete decolourization of rhodamine B dye within 15 min (Basavegowda et al. 2017).

6 Remediation Potential of Phyto-Nanoparticles in Wastewater Treatment

6.1 Dye Degradation from Wastewater

Heterogeneous photocatalysis is technique used for purification of wastewater. The mechanism can be classified based upon the type of catalyst. Photo-decolouration involves photo-oxidation and photo-reduction in which dye converted to its original form. Photo-degradation converted the dye into some non-toxic stable product. Photo-mineralization gives the potential to decompose the dye into carbon dioxide, water, nitrate, etc.. Photo-decomposition involves photo-degradation and photo-mineralization. In photocatalytic degradation of dye, excited electron moves from valence band to conductance band, generating electron hole pair which result in oxidative photo-degradation by generating the hydroxyl radical. thus, atmospheric oxygen comes in contact with electron resulting in complete degradation of dye to non-toxic by products such as carbon dioxide, water molecule, etc. (Marimuthu et al. 2020). TiO_2 can be used as potent oxidizing agent because of its high energy gap between valance band and conductance band. A suitable metal which is stable, act as good conductor as well as absorbs light easily can be doped with TiO_2 to reduce the energy gap. Electron captured by oxygen in water forming a free radical. Hole

created by due to excitation of electron finally accepts the electron from absorbed dye resulting in reduction of dye. Determination of dye degradation through UV-Vis spectroscopy carried out by evaluating the optical density of nanoparticles. The electron transfer from donor to acceptor held on the surface of nanoparticle thus, it acts as a catalyst for the reaction. The dye degradation is dependent upon the size and shape of synthesized nanoparticle and the target dye chemical structure. Silver and palladium nanoparticle synthesized from *Daucus carota* leaf extract shows high efficiency of removing rhodamine 6-G dye. Catalytic property was evaluated that came to be 98% and 89.4% of rhodamine dye get decolourized within 2 min and 30 min under the treatment of palladium nanoparticle and silver nanoparticle respectively (Joseph Kirubaharan et al. 2020). Silver nanoparticle synthesized from *Albizia procera* shows promising results in removing methyl blue dye. Optimized pH at 11.5 to get removal efficiency of 99.6% of methyl blue dye. Similarly, temperature optimized at 30 degree Celsius and contact time of around 70 min to get removal efficiency of 93.65% and 51.54% respectively (Rafique et al. 2019). Green synthesis of copper nanoparticle is successful in degrading 96% of methyl blue dye from aqueous solution under optimize conditions (Sinha and Ahmaruzzaman 2015). Several studies conducted on applicability of plant-based nanomaterials for dyes and heavy metal pollution, UV–Vis range for dye degradation analysis, and additives etc., have been presented in Table 3.

6.2 Heavy Metal Removal from Aqueous Solution

Adsorption mechanism assisted by electrostatic interaction, complexation and adsorbent nature. electrostatic interaction between metal ion and adsorbent are driving forces for adsorption process (Sarma et al. 2019). plant mediated nanoparticles provide a function group which increases in binding site and form surface complex by electrostatic attraction. Adsorbate interaction with adsorbent determines with the help of different isotherm include Freundlich isotherm and Langmuir isotherm. Kinetic model include pseudo first order reaction and pseudo second order reaction helps in determining the type of adsorption on adsorbent along with reaction pathways. combination of theoretical and experimental calculation obtained from adsorption isotherms and kinetic model explain the efficient removal of heavy metal from the water (Al-Senani and Al-Fawzan 2018). Adsorption capacity of silicon nanoparticle synthesized from plant extracted *Saccharum ravannae, Saccharum officinarum* and *Oryza sativa* found to be above 95% for Pb^{2+} and Ca^{2+}. The adsorption studies of Silica nanoparticle is done by optimizing various parameters like pH, metal ion concentration, temperature, adsorbent dose and contact (Sachan et al. 2021). The adsorption mechanism is understood by various isotherm models like Freundlich isotherm and Langmuir isotherm and thermodynamic studies. Iron nanoparticle synthesized by using tea extract was irradiated with ^{60}Co gamma radiation. The adsorption capacity of Cu^{2+} ions in aqueous solution before and after radiation was observed 81.67% and 97% respectively under optimize condition (Amin et al. 2021).

Table 3 Phytonanoparticles showing removal efficiency of heavy metals and dye degradation from aqueous solution

Nanoparticle	Heavy metal/dye	UV- Vis of dye/NP (obs.)	Reaction time	Additives	pH	Percentage removal/observation	References
Silver nanoparticle	Methylene blue dye	660 nm/420 nm	0–72 h	–	5.6 6.6 7.6 8.6	95.3% at 72 h at 8.6 pH	Vanaja et al. (2014)
Silver nanoparticle	Congo red dye	SPR band—498 (pie-pie) 338(n-pie)	At interval of 1.5 min upto 15 min	Sodium borohydride	–	Not given	Kolya et al. (2015)
Silver nanoparticle	Congo red dye	496 nm dye/426 AgNP	0–13 mintues	Sodium borohydride	–	98.5 upto 5 cycles	Chand et al. (2021)
Silver nanoparticle	Safranin O Methyl red, Methyl Orange, Methyl blue (10 mg/l)	519 nm 415 nm 460 nm 664 nm (AgNP- 419 nm)	0–24 h	–	–	**Degradation rate constant** 1.02×10^{-3}/min 1.03×10^{-3} 1.86×10^{-3} 1.44×10^{-3}	Jyoti and Singh (2016)
Silver nanoparticle	Brilliant blue Tartrazine Carmoisine	629 nm 420 nm 504 nm	**Reaction rate constant-k** 0.2097 0.0076 0.0496	Sodium borohydride	–	–	David and Moldovan (2020)

(continued)

Table 3 (continued)

Nanoparticle	Heavy metal/dye	UV- Vis of dye/NP (obs.)	Reaction time	Additives	pH	Percentage removal/observation	References
Silver nanoparticle	Methyl blue Methyl orange	500–700 350–550 nm	1 mM 5 min 2 mM–5 min 1 mM 5 min 2 mM 5 min	Sodium borohydride	–	27.12% 18.08% 69.79% 42.11%	Chandra Paul et al. (2020)
Silver nanoparticle	Hg2 + detection	Not mentioned (given a graph)	–	–	pH- 3–8 (no effect of pH)	Dark yellow changes to colourless	Roy et al. (2015)
Silver nanoparticle	Detection of Hg2+	Not mention (graph given)	–	–	–	Dark brown changes to colourless	Tagad et al. (2017)
Gold nanoparticle	Toxic metal removal Pd Cd Cu Fe Ni Co Mn Zn Pb	Absorption capacity of adsorbent used in aqueous soln. of toxic metal was determined by batch method	120 min	–	5 6 6.5	Removal% 63.46 60.20 51.50 68.20 42.18 23.47 21.62 35.37 75.76	Baran et al. (2020b)

(continued)

Table 3 (continued)

Nanoparticle	Heavy metal/dye	UV- Vis of dye/NP (obs.)	Reaction time	Additives	pH	Percentage removal/observation	References
SnO_2 nanoparticle	Photodegradation of RhB Removal of heavy metal Co + 2	553.5/370–375 nm	190 min 60 min	–	7 >7 >8	91.7% Adsorption capacity 93.6% Formation of soluble hydroxyl complex in excess of OH Cobalt hydroxide started to ppt from aq. Sol. & adsorption was impossible	Ebrahimian et al. (2020)
Zero valent iron nanoparticle	Adsorption of Cr(VI)	–	30 min 90 min	Oenothein B	–	Adsorption efficiency 98.1% 71.9%	Madhavi et al. (2013a)
Maghemite nanoparticle	Removal of heavy metal in fly ash Pb Cd	–	1 h 24 h 1 h 24 h	–	7	85.56% 90.85% 67.8% Conc. Reached below the detection level of ICP-OES (not defined)	Yadav and Fulekar (2018a)

(continued)

Table 3 (continued)

Nanoparticle	Heavy metal/dye	UV- Vis of dye/NP (obs.)	Reaction time	Additives	pH	Percentage removal/observation	References
Iron based nanoparticle	Removal of Cr (VI) and Cu (II) when co-existed together Cr (VI) and Cu (II) present separately Removal efficiency of Cr Cu (II) Pb (II) Zn (II)	– –	1 h T = 288 K T = 308 K	–	5	Cr (VI)- 58.9% Cu (II)-33% Cr (VI) = 74.2%; Cu (II) = 45.2% Cu-26.8% Cr-50.7% Cu-40.8% Cr-62.6% Cr = from 75.1% to 50.8% Cu 28.3% to 64.2% 44.8 21.5 31.4 10.8	Ajitha et al. (2015)
Zero valent Silver nanoparticle	Cadmium removal from aqueous solution	–	40 min	–	6	85% 75.5%	Al-Qahtani (2017)
Zero valent iron nanoparticles	Removal of Cr (VI) from aqueous solution **TV-Fe** (higher% removal) UD-Fe RD-Fe	Adsorption capacities 466 462 453.7	1–10 1–10 30 min	–	2–9	91.75% 60.95% 97.5% 97.1% 96.94%	Fazlzadeh et al. (2017)
Silver nanoparticles	Chromium removal	350 nm	–	Activated carbon	–	Absorbing pattern was irregular	Samrot et al. (2019)

Iron oxide nanoparticles synthesized from *Ramalina sinesis* extract was successfully able to remove lead and cadmium by following Langmuir adsorption isotherm and Freundlich adsorption isotherm respectively also both removal follows second order kinetic model with removal capacity of 82% for lead and 77% for cadmium under the pH ranges between 4 to 5 and initial ion concentration was 50 mg/l with 70-degree temperature in 1 h (Arjaghi et al. 2021).

Factor Affecting Removal of Heavy Metal

Biomass concentration

Increase in biomass concentration results in increases in number of metal binding sites hence increase adsorption efficiency. Lead, zinc and chromium removal efficiency increases from 94.35% to 100%, 44% to 36.9% and 55% to 81.9% respectively, when concentration of biomass changes from 0.2 g to 2 g (Chandra Sekhar et al. 2003). At very high concentration of biomass, metal removal efficiency decreases because of the reduction average distance available for absorption sites due to the aggregation of biomass. Copper uptake efficiency decreases from 85 to 58%. With increased biosorption concentration from 0.5 g/l to 2 g/l (Chandra Sekhar et al. 2003). From comparative studies, we can conclude that low biomass concentration results in decreased biosorption efficiency. With increase in dosage of zerovalent iron nanoparticle from 0.5 g/l to 2.0 g/l, the removal efficacy of Cu, Zn, Cr and Pb was increased from 76%, 14% 51% and 78% to more than 80% in both Zn and Pb followed by complete removal of Cu and Cr within 30 min. higher pH was obtained at higher biomass concentration for the removal of heavy metal like Zn, Pb, Cr and Cu (Chen et al. 2008). Since metal removal occurs at the surface of the nanoparticle, the maximum removal of heavy metal become unchanged. Also, removal efficiency of heavy metal is inversely proportional to the initial metal ion concentration under a constant biomass concentration. Magnetite concentration was increased from 1 g/l to 4 g/l in order to increases the removal efficiency of hexavalent chromium from 29.1% to complete removal (Ataabadi et al. 2015).

p^H

The important factor is pH, affecting the chemistry of metal ions and biosorbent by influencing their solubility as well as toxicity. Metal uptake related to complexation chemistry of metal ion and behaviour of function group present at the surface of the plant. The carbonyl group of biomolecule provide a negative charge at acidic condition due to which an electrostatic interaction occurs between two cationic which results in biosorption of metal. At low pH, H + ions are occupied in the active sites of adsorption, with increases in pH these sites become free and available for the heavy metal on the surface of adsorbent. In the pH range of 3–7 there is slight increase in removal process of heavy metal like Cr(VI) removal favoured at low pH due to the positive charged surface of nanoparticle at low pH attract the negative charge anions as a result an electrostatic attraction occurred (Weng et al. 2016b). Also, at some point

adsorption sites become independent of pH change indicating saturation point which is attributed to formation of hydroxyl complex in excess of OH ion, depends upon the type of heavy metal that is to be removed and the surface of nanoparticle. Adsorption capacity increases with increases in pH until it attains a maximum biosorption at optimum pH because further increase in pH will result in precipitation of metal. Addition of NaOH and HNO_3 leads to increment and reduction of pH respectively. Studies have been be conducted over silver nanoparticle synthesis from different plant extract like neem leaf, sun dried leaf of neem, neem bark, mango leaf, sun dried leaf of mango, green tea and pepper seed extract selectively sense heavy metal like mercury, lead, zinc, cobalt and zinc over a wide range of pH from initial pH and highest pH that maintains acidic and basic environment respectively. At initial pH 4, mercury was detected by neem bark synthesized silver nanoparticle but it was not detected when increasing the pH up to 9 rest other metal like cobalt and nickel was detected (Karthiga and Anthony 2013).

Temperature

Higher temperature increases the solubility of metal ion in water, therefore biosorption of these metal ions become difficult. Temperature depends upon the type of chemical reaction occurring between biosorbent and metal ion. Metal removal efficiency decreases with increase temperature for exothermic biosorption as the absorption of the molecule becomes easier and when temperature rise, desorption of the molecule take place. Sorption of lead and cadmium by Caladium bicolor biomass is affected between 30 to 80 degrees Celsius. Increase in temperature results in weak attractive forces between bisorbent and bisorbate, thinning of the outer boundary layer which help the metal ion which lead to decreases in sorption. Lower temperature helps in enhancing the activation energy and solubility of chemical to increase the rate of the reaction. Uptake of lead ion to biosorbent by peanut shell effectively remove 66% of lead at 20 degrees Celsius. Removal efficiency decreases with increase in temperature from 20 degree Celsius to 40 degree Celsius showed exothermic biosorption (Taşar et al. 2014). In zinc oxide nanoparticle, increase in temperature from 30 to 70-degree result in increase in adsorption capacity of lead from 16.19 mg/g to 19.96 mg/g (Azizi et al. 2017) whereas increase in temperature from 288 to 308 K results in higher adsorption of Cr (VI) and Cu (II) on the surface of iron nanoparticle (Weng et al. 2016b). Interaction between available sites of the absorbent with absorbate efficiently increases the removal rate from 73.8% to 100% of the toxic hexavalent chromium with increase in temperature from 25 degrees Celsius to 40 degrees Celsius respectively (Ataabadi et al. 2015). Therefore, temperature depends upon the nature of the process.

Initial metal ion concentration

Adsorption capacity increases with initial metal ion concentration. When all binding sites occupied with metal result in increase in concentration slope. There would be decrease in adsorption rate with further increasing the concentration of metal ion as all the obtainable nanoparticle sites are filled. Removal efficiency of chromium is 86% with initial iron concentration 30 mg/l. increase in iron concentration up to

150 mg/l result in deduce the adsorption efficiency from 86 to 70% (Al-Qahtani 2017). 100 mg/ml is the concentration of metal ion where the removal efficiency of chromium is highest that is 42.37%. Further increasing the metal ion concentration up to 200 mg/ml, the removal efficiency of chromium decreased from 42.37% to 33.75% as all available site occupied which result in closing of the pores and hence metal ion preventing penetrating deep into adsorbent pore (Shaik et al. 2020b). Zerovalent iron nanoparticle effectively remove hexavalent chromium with adsorption efficiency of 98.1% observed within 30 min when initial metal ion concentration is 200 mg/ml. adsorption efficiency decreases to 71.9% with increase in metal ion concentration up to 400 mg/ml (Madhavi et al. 2013b).

Contact time

Contact time indirectly effects the rate of adsorption and the data was analysed by kinetic models namely pseudo first order and pseudo second order model. It has similar affect as of initial metal concentration, biosorption increases with increase in contact time. When all the binding sites become fully saturated, the reaction become independent of time. Cadmium removal from aqueous solution carried out at optimum contact time of 40 min. over that time, no further increase in cadmium removal efficiency (Al-Qahtani 2017). Absorption capacity of hexavalent chromium decreases from 98.1% to 72.9% with increase in contact time of 30 min to 90 min (Madhavi et al. 2013b). Maghemite nanoparticle effectively remove lead and cadmium from fly ash with respect to time. The removal process observed upto 0 to 24 h. It has been observed that initially, 85.56% of lead is removed and cadmium removal was not defined by ICP-OES. After 2 h, 67.8% removal of cadmium was detected followed by detection of 90.85% lead at 24 h (Yadav and Fulekar 2018b). Most of the adsorption site are occupied initially that's why it attains an equilibrium and removal percentage does not increase rapidly.

6.3 Desorption Analysis

Desorption studies refer to the removal of absorbed metal from the surface of absorbent. There are various types of desorbing agents including tap water, sodium hydroxide, hydrochloric acid, deionized water, sulphuric acid, ammonium hydroxide, potassium hydroxide. For example, the desorption efficiency of HCl and H_2SO_4 is very high in removing the Cr (VI) and Pb (II) ions respectively from the adsorbent. It was found that adsorbent exhibited good removal efficiency of chromium and lead up to five consecutive cycles (Bayuo et al. 2020). Sodium hydroxide is considered best for the removal of chromium up to five consecutive cycles as its desorption efficacy reduces from 98 to 89% after the fifth cycle (Al-Haddad et al. 2020). Chromium desorption from red peanut skin synthesized iron nanoparticle was done by using 16 M hydrochloric acid and distilled water as desorbents. Iron nanoparticle dried by vacuum under 40 degrees Celsius and 60 degrees Celsius as well as air dried at room temperature. Maximum chromium efficiency that is 100% within 1 min was achieved

by vacuum dried at 60 degrees Celsius then followed by vacuum dried iron nanoparticle at 40 degrees Celsius. It has been hypothesized that with increase in temperature of vacuum drying, reduction of radius of iron nanoparticle occurred due to which at higher temperature chromium removal occurred more rapidly. Minimum removal efficiency was 90% in 4.5 h given by air dried iron nanoparticle due to formation of ferrosoferric oxide (Pan et al. 2019). Bimetallic silver- copper nanoparticle at zinc oxide surface efficiently able to degrade rhodamine B to leuco rhodamine B dye and Congo red dye within 12 s and 9 s respectively up to five consecutive cycles because after that leaching of metal started which can be determined by ICP-AES (Manjari et al. 2020).

7 Challenges and Future Prospects

Nanoparticles have been successfully found active in remediating the waste water but at the same time, they also face some critical challenges in their synthesis. Since we discussed the green synthesis of nanoparticle, first of all there is need for the selection of appropriate plants which are rich in phytocompounds like polyphenol, flavonoids, terpenoids, alkaloids etc. Identification of particular biochemical compound present in the plant that acts as a reducing capping and stabilising agent of the nanoparticle is also necessary. After selection of suitable plant with exact targeted active phytochemical compound, the selection of suitable metal precursor is needed. Nanoparticles have small size and larger surface area due to which they have more interaction sites available on their surface with cells. This gives several toxic biological responses. Smaller the size of the nanoparticle, greater the toxicity attributed with it. Toxicity of nanoparticle depends upon various parameters including structure, shape, hydrophilicity, composition, concentration, reaction temperature and surface chemistry. The toxicological effects of nanoparticle affect humans and environment. Acute and chronic toxicity occur upon oral exposure of several metal nanoparticles. Due to their small size, some nanoparticles pass the blood brain barrier which may lead to dangerous neural diseases. Reuse of nanoparticles is another challenge.

Nanotechnology is establishing in every field, be it agricultural engineering, drug delivery, X-ray imaging, dentistry, cosmetics or other environmental aspects. From past studies, we can conclude that nanoparticle synthesis by traditional methods requires heavy machine equipment and toxic chemicals with complex handling which is a very costly procedure. To overcome these disadvantages, we moved to green synthesis of nanoparticles from plant, algae, bacteria and fungi. This chapter presents an insight into nanoparticle synthesis from plant extract. Exact mechanism of the targeted biochemical process occurs at cellular level for increased production of nanoparticle, which can be discovered in further studies. More studies can be carried out on capping agents which prevent the further reaction aggregation and result in providing stability for a longer period of time. We have to expand the area of the sources of nanoparticle synthesis so that they can be synthesized from waste materials like algae and several other plants which are cheap, easily

available and suitable. Very limited studies have been carried out on the toxicity of phyto-nanoparticles. We need to develop several strategies for detoxification of green nanoparticles. Research cannot be restricted to water pollutant removal only. We can explore new opportunities in the environmental air purification also, to reduce the amount of particulate matter (PM), ozone, sulphur, etc.

8 Conclusion

Pollutants such as heavy metal and various organic or synthetic dyes contaminate the water bodies leading to water pollution thus creating many problems related to human and animal health and affecting the environment. Therefore, there is an immediate requirement of water treatment. Phyto-nanotechnology holds an enormous potential to remediate wastewater as it offers inexpensive, eco-friendly and efficient way. In this chapter, we have discussed the various types of plant synthesized nanoparticles which can be used to remediate wastewater. The exploration of biotechnological prospects for nanoparticles synthesis at industrial scale remediation of wastewater is needed. The article concludes that phytonanoparticles can be a potential, inexpensive and ecofriendly agents for environmental pollution remediation.

Declarations **Funding**: Not Applicable.

Conflicts of Interest: The authors declare that they have no conflict of interest.

Availabity of data and material: Not Applicable.

Code Availability: Not Applicable.

References

Ajitha B, Ashok Kumar Reddy Y, Sreedhara Reddy P (2015) Green synthesis and characterization of silver nanoparticles using Lantana camara leaf extract. Mater Sci Eng C 49:373–381. https://doi.org/10.1016/j.msec.2015.01.035

Al-Haddad J, Alzaabi F, Pal P et al (2020) Green synthesis of bimetallic copper–silver nanoparticles and their application in catalytic and antibacterial activities. Clean Technol Environ Policy 22:269–277. https://doi.org/10.1007/s10098-019-01765-2

Al-Qahtani KM (2017) Cadmium removal from aqueous solution by green synthesis zero valent silver nanoparticles with Benjamina leaves extract. Egypt J Aquat Res 43:269–274. https://doi.org/10.1016/j.ejar.2017.10.003

Al-Senani GM, Al-Fawzan FF (2018) Adsorption study of heavy metal ions from aqueous solution by nanoparticle of wild herbs. Egypt J Aquat Res 44:187–194. https://doi.org/10.1016/j.ejar.2018.07.006

Amaliyah S, Pangesti DP, Masruri M, Sabarudin A, Sumitro SB (2020) Green synthesis and characterization of copper nanoparticles using Piper retrofractum Vahl extract as bioreductor and capping agent. Heliyon 6:e04636. https://doi.org/10.1016/j.heliyon.2020.e04636

Amin RM, Mahmoud RK, Gadelhak Y, El-Ela FIA (2021) Gamma irradiated green synthesized zero valent iron nanoparticles as promising antibacterial agents and heavy metal nano-adsorbents. Environ Nanotechnol Monit Manag, 100461.https://doi.org/10.1016/j.enmm.2021.100461

Antony D, Yadav R (2021) Facile fabrication of green nano pure CeO_2 and Mn-decorated CeO_2 with Cassia angustifolia seed extract in water refinement by optimal photodegradation kinetics of malachite green. Environ Sci Pollut Res 28:18589–18603. https://doi.org/10.1007/s11356-020-11153-9

Arjaghi SK, Alasl MK, Sajjadi N et al (2021) Green synthesis of iron oxide nanoparticles by RS lichen extract and its application in removing heavy metals of lead and cadmium. Biol Trace Elem Res 199:763–768. https://doi.org/10.1007/s12011-020-02170-3

Ataabadi M, Hoodaji M, Tahmourespour A, et al (2015) Optimization of factors affecting hexavalent chromium removal from simulated electroplating wastewater by synthesized magnetite nanoparticles. Environ Monit Assess, 187.https://doi.org/10.1007/s10661-014-4165-z

Azizi S, Shahri MM, Mohamad R (2017) Green synthesis of zinc oxide nanoparticles for enhanced adsorption of lead Ions from aqueous solutions: equilibrium, kinetic and thermodynamic studies. Molecules, 22https://doi.org/10.3390/molecules22060831

Babuponnusami A, Muthukumar K (2014) A review on Fenton and improvements to the Fenton process for wastewater treatment. J Environ Chem Eng 2:557–572. https://doi.org/10.1016/j.jece.2013.10.011

Badmapriya D, Asharani IV (2016) Dye degradation studies catalysed by green synthesized iron oxide nanoparticles. Int J ChemTech Res 9:409–416

Baran MF, Acay H, Keskin C (2020a) Saponaria officinalis determination of antimicrobial and toxic metal removal activities of plant-based synthesized (Capsicum annuum L. Leaves), ecofriendly, gold nanomaterials, Glob. Challenges 4:1900104. https://doi.org/10.1002/gch2.201900104

Baran MF, Acay H, Keskin C (2020b) Determination of antimicrobial and toxic metal removal activities of plant-based synthesized (Capsicum annuum L. Leaves), ecofriendly, gold nanomaterials. Glob Challenges 4:1900104. https://doi.org/10.1002/gch2.201900104

Barberia-Roque L, Gámez-Espinosa E, Viera M, Bellotti N (2019) Assessment of three plant extracts to obtain silver nanoparticles as alternative additives to control biodeterioration of coatings. Int Biodeterior Biodegrad 141:52–61. https://doi.org/10.1016/j.ibiod.2018.06.011

Basavegowda N, Mishra K, Lee YR (2017) Trimetallic FeAgPt alloy as a nanocatalyst for the reduction of 4-nitroaniline and decolorization of rhodamine B: a comparative study. J Alloys Compd 701:456–464. https://doi.org/10.1016/j.jallcom.2017.01.122

Bayuo J, Abukari MA, Pelig-Ba KB (2020) Desorption of chromium (VI) and lead (II) ions and regeneration of the exhausted adsorbent. Appl Water Sci 10:1–6. https://doi.org/10.1007/s13201-020-01250-y

Bibi I, Kamal S, Ahmed A, Iqbal M, Nouren S, Jilani K, Nazar N, Amir M, Abbas A, Ata S, Majid F (2017) Nickel nanoparticle synthesis using Camellia Sinensis as reducing and capping agent: Growth mechanism and photo-catalytic activity evaluation. Int J Biol Macromol 103:783–790. https://doi.org/10.1016/j.ijbiomac.2017.05.023

Bibi I, Nazar N, Ata S, Sultan M, Ali A, Abbas A, Jilani K, Kamal S, Sarim FM, Khan MI, Jalal F, Iqbal M (2019) Green synthesis of iron oxide nanoparticles using pomegranate seeds extract and photocatalytic activity evaluation for the degradation of textile dye. J Mater Res Technol 8:6115–6124. https://doi.org/10.1016/j.jmrt.2019.10.006

Binod A, Ganachari S V, Yaradoddi JS et al (2018) Biological synthesis and characterization of trimetallic alloy (Au Ag, Sr) nanoparticles and its sensing studies. IOP Conf Ser Mater Sci Eng 376.https://doi.org/10.1088/1757-899X/376/1/012054

Bishnoi S, Kumar A, Selvaraj R (2018) Facile synthesis of magnetic iron oxide nanoparticles using inedible Cynometra ramiflora fruit extract waste and their photocatalytic degradation of methylene blue dye. Mater Res Bull 97:121–127. https://doi.org/10.1016/j.materresbull.2017.08.040

Chand K, Jiao C, Lakhan MN, Shah AH, Kumar V, Fouad DE, Chandio MB, Ali Maitlo A, Ahmed M, Cao D (2021) Green synthesis, characterization and photocatalytic activity of silver nanoparticles

synthesized with Nigella Sativa seed extract. Chem Phys Lett 763:138218. https://doi.org/10.1016/j.cplett.2020.138218
Chandra Paul S, Bhowmik S, Rani Nath M, Islam MS, Kanti Paul S, Neazi J, Sabnam Binta Monir T, Dewanjee S, Abdus Salam M (2020) Silver nanoparticles synthesis in a green approach: size dependent catalytic degradation of cationic and anionic dyes, orient. J Chem 36:353–360. https://doi.org/10.13005/ojc/360301
Chandra Sekhar K, Kamala CT, Chary NS, Anjaneyulu Y (2003) Removal of heavy metals using a plant biomass with reference to environmental control. Int J Miner Process 68:37–45. https://doi.org/10.1016/S0301-7516(02)00047-9
Chelly M, Chelly S, Zribi R, Bouaziz-ketata H, Gdoura R, Lavanya N, Veerapandi G, Sekar C, Neri G (2021) Synthesis of silver and gold nanoparticles from rumex roseus plant extract and their application in electrochemical sensors. Nanomaterials 11:1–18. https://doi.org/10.3390/nano11030739
Chen SY, Chen WH, Shih CJ (2008) Heavy metal removal from wastewater using zero-valent iron nanoparticles. Water Sci Technol 58:1947–1954. https://doi.org/10.2166/wst.2008.556
Chowdhury S, Mazumder MAJ, Al-Attas O, Husain T (2016) Heavy metals in drinking water: occurrences, implications, and future needs in developing countries. Sci Total Environ 569–570:476–488. https://doi.org/10.1016/j.scitotenv.2016.06.166
David L, Moldovan B (2020) Green synthesis of biogenic silver nanoparticles for efficient catalytic removal of harmful organic dyes. Nanomaterials 10. https://doi.org/10.3390/nano10020202
Dlugaszewska J, Dobrucka R (2019) Effectiveness of biosynthesized Trimetallic Au/Pt/Ag nanoparticles on planktonic and biofilm enterococcus faecalis and enterococcus faecium Forms. J Clust Sci 30:1091–1101. https://doi.org/10.1007/s10876-019-01570-3
Dobrucka R (2019) Facile synthesis of trimetallic nanoparticles Au/CuO/ZnO using Vitex agnus-castus extract and their activity in degradation of organic dyes. Int J Environ Anal Chem 00:1–12. https://doi.org/10.1080/03067319.2019.1691543
Dubey S, Sharma YC (2017) Calotropis procera mediated one pot green synthesis of Cupric oxide nanoparticles (CuO-NPs) for adsorptive removal of Cr(VI) from aqueous solutions. Appl Organomet Chem 31:1–15. https://doi.org/10.1002/aoc.3849
Ebrahimian J, Mohsennia M, Khayatkashani M (2020) Photocatalytic-degradation of organic dye and removal of heavy metal ions using synthesized SnO_2 nanoparticles by Vitex agnus-castus fruit via a green route. Mater Lett 263:127255. https://doi.org/10.1016/j.matlet.2019.127255
Ebrahiminezhad A, Taghizadeh S, Ghasemi Y, Berenjian A (2018) Green synthesized nanoclusters of ultra-small zero valent iron nanoparticles as a novel dye removing material. Sci Total Environ 621:1527–1532. https://doi.org/10.1016/j.scitotenv.2017.10.076
Ehrampoush MH, Miria M, Salmani MH, Mahvi AH (2015) Cadmium removal from aqueous solution by green synthesis iron oxide nanoparticles with tangerine peel extract. J Environ Heal Sci Eng 13:1–7. https://doi.org/10.1186/s40201-015-0237-4
Fazlzadeh M, Rahmani K, Zarei A, Abdoallahzadeh H, Nasiri F, Khosravi R (2017) A novel green synthesis of zero valent iron nanoparticles (NZVI) using three plant extracts and their efficient application for removal of Cr(VI) from aqueous solutions. Adv Powder Technol 28:122–130. https://doi.org/10.1016/j.apt.2016.09.003
Fernandez AC, KM A, Rajagopal R (2020) Green synthesis, characterization, catalytic and antibacterial studies of copper iodide nanoparticles synthesized using Brassica oleracea var. capitata f. rubra extract. Chem Data Collect 29:100538. https://doi.org/10.1016/j.cdc.2020.100538
Fowsiya J, Madhumitha G, Al-Dhabi NA, Arasu MV (2016) Photocatalytic degradation of Congo red using Carissa edulis extract capped zinc oxide nanoparticles. J Photochem Photobiol B Biol 162:395–401. https://doi.org/10.1016/j.jphotobiol.2016.07.011
Glossman-Mitnik D (2013) Computational study of the chemical reactivity properties of the Rhodamine B molecule. Procedia Comput Sci 18:816–825. https://doi.org/10.1016/j.procs.2013.05.246

Gopal G, Sankar H, Natarajan C, Mukherjee A (2020) Tetracycline removal using green synthesized bimetallic nZVI-Cu and bentonite supported green nZVI-Cu nanocomposite: a comparative study. J Environ Manage 254:109812. https://doi.org/10.1016/j.jenvman.2019.109812

Gopalakrishnan V, Muniraj S (2021) Neem flower extract assisted green synthesis of copper nanoparticles—optimisation, characterisation and anti-bacterial study. Mater Today Proc 36:832–836. https://doi.org/10.1016/j.matpr.2020.07.013

Goutam SP, Saxena G, Singh V, Yadav AK, Bharagava RN, Thapa KB (2018) Green synthesis of TiO_2 nanoparticles using leaf extract of Jatropha curcas L. for photocatalytic degradation of tannery wastewater. Chem Eng J 336:386–396. https://doi.org/10.1016/j.cej.2017.12.029

Groiss S, Selvaraj R, Varadavenkatesan T, Vinayagam R (2017) Structural characterization, antibacterial and catalytic effect of iron oxide nanoparticles synthesised using the leaf extract of Cynometra ramiflora. J Mol Struct 1128:572–578. https://doi.org/10.1016/j.molstruc.2016.09.031

Guerra FD, Attia MF, Whitehead DC, Alexis F (2018) Nanotechnology for environmental remediation: materials and applications. Molecules 23:1–23. https://doi.org/10.3390/molecules23071760

Guo B, Li M, Li S (2020) The comparative study of a homogeneous and a heterogeneous system with green synthesized iron nanoparticles for removal of Cr(VI). Sci Rep 10:1–11. https://doi.org/10.1038/s41598-020-64476-5

Hao R, Li D, Zhang J, Jiao T (2021) Green synthesis of iron nanoparticles using green tea and its removal of hexavalent chromium. Nanomaterials 11:1–13. https://doi.org/10.3390/nano11030650

Hassan AK, Al-Kindi GY, Ghanim D (2020) Green synthesis of bentonite-supported iron nanoparticles as a heterogeneous Fenton-like catalyst: kinetics of decolorization of reactive blue 238 dye. Water Sci Eng 13:286–298. https://doi.org/10.1016/j.wse.2020.12.001

Ismail M, Akhtar K, Khan MI, Kamal T, Khan MA, Asiri AM, Seo J, Khan SB (2019) Pollution, toxicity and carcinogenicity of organic dyes and their catalytic bio-remediation. Curr Pharm Des 25:3645–3663. https://doi.org/10.2174/1381612825666191021142026

Jayachandran A, ATR, Nair AS (2021) Green synthesis and characterization of zinc oxide nanoparticles using Cayratia pedata leaf extract. Biochem Biophys Reports 26:100995. https://doi.org/10.1016/j.bbrep.2021.100995

Jha AK, Chakraborty S (2020) Photocatalytic degradation of Congo Red under UV irradiation by zero valent iron nano particles (nZVI) synthesized using Shorea robusta (Sal) leaf extract. Water Sci Technol 82:2491–2502. https://doi.org/10.2166/wst.2020.517

Joseph Kirubaharan C, Fang Z, Sha C, Yong YC (2020) Green synthesis of Ag and Pd nanoparticles for water pollutants treatment. Water Sci Technol 82:2344–2352. https://doi.org/10.2166/wst.2020.498

Jyoti K, Singh A (2016) Green synthesis of nanostructured silver particles and their catalytic application in dye degradation. J Genet Eng Biotechnol 14:311–317. https://doi.org/10.1016/j.jgeb.2016.09.005

Karthiga D, Anthony SP (2013) Selective colorimetric sensing of toxic metal cations by green synthesized silver nanoparticles over a wide pH range. RSC Adv 3:16765–16774. https://doi.org/10.1039/c3ra42308e

Khan M, Al-Hamoud K, Liaqat Z et al (2020) Synthesis of au, ag, and au–ag bimetallic nanoparticles using pulicaria undulata extract and their catalytic activity for the reduction of 4-nitrophenol. Nanomaterials 10:1–14. https://doi.org/10.3390/nano10091885

Khan SA, Shahid S, Ayaz A, Alkahtani J, Elshikh MS, Riaz T (2021) Phytomolecules-coated NiO nanoparticles synthesis using abutilon indicum leaf extract: antioxidant, antibacterial, and anticancer activities. Int J Nanomedicine 16:1757–1773. https://doi.org/10.2147/IJN.S294012

Khan ZUH, Sadiq HM, Shah NS, Khan AU, Muhammad N, Hassan SU, Tahir K, safi SZ, Khan FU, Imran M, Ahmad N, Ullah F, Ahmad A, Sayed M, Khalid MS, Qaisrani SA, Ali M, Zakir M (2019) Greener synthesis of zinc oxide nanoparticles using Trianthema portulacastrum extract

and evaluation of its photocatalytic and biological applications. J Photochem Photobiol B Biol 192:147–157. https://doi.org/10.1016/j.jphotobiol.2019.01.013

Khunjan U, Kasikamphaiboon P (2021) Green synthesis of kaolin-supported nanoscale zero-valent iron Using Ruellia tuberosa leaf extract for effective decolorization of azo dye reactive black 5. Arab J Sci Eng 46:383–394. https://doi.org/10.1007/s13369-020-04831-w

Kolya H, Maiti P, Pandey A, Tripathy T (2015) Green synthesis of silver nanoparticles with antimicrobial and azo dye (Congo red) degradation properties using Amaranthus gangeticus Linn leaf extract. J Anal Sci Technol 6:4–10. https://doi.org/10.1186/s40543-015-0074-1

Krishnaraj C, Jagan EG, Rajasekar S, Selvakumar P, Kalaichelvan PT, Mohan N (2010) Synthesis of silver nanoparticles using Acalypha indica leaf extracts and its antibacterial activity against water borne pathogens. Colloids Surfaces B Biointerfaces 76:50–56. https://doi.org/10.1016/j.colsurfb.2009.10.008

Kuang Y, Wang Q, Chen Z, Megharaj M, Naidu R (2013) Heterogeneous Fenton-like oxidation of monochlorobenzene using green synthesis of iron nanoparticles. J Colloid Interface Sci 410:67–73. https://doi.org/10.1016/j.jcis.2013.08.020

Kushwaha AK, Gupta N, Chattopadhyaya MC (2014) Removal of cationic methylene blue and malachite green dyes from aqueous solution by waste materials of Daucus carota. J Saudi Chem Soc 18:200–207. https://doi.org/10.1016/j.jscs.2011.06.011

Lellis B, Fávaro-Polonio CZ, Pamphile JA, Polonio JC (2019) Effects of textile dyes on health and the environment and bioremediation potential of living organisms. Biotechnol Res Innov 3:275–290. https://doi.org/10.1016/j.biori.2019.09.001

Lü F, Gao Y, Huang J, Sun D, Li Q (2014) Roles of biomolecules in the biosynthesis of silver nanoparticles: case of gardenia jasminoides extract, Chinese. J Chem Eng 22:706–712. https://doi.org/10.1016/S1004-9541(14)60086-0

Luo F, Yang D, Chen Z et al (2016a) Characterization of bimetallic Fe/Pd nanoparticles by grape leaf aqueous extract and identification of active biomolecules involved in the synthesis. Sci Total Environ 562:526–532. https://doi.org/10.1016/j.scitotenv.2016.04.060

Luo F, Yang D, Chen Z, Megharaj M, Naidu R (2016b) One-step green synthesis of bimetallic Fe/Pd nanoparticles used to degrade Orange II. J Hazard Mater 303:145–153. https://doi.org/10.1016/j.jhazmat.2015.10.034

Madhavi V, Prasad TNVKV, Reddy AVB, Ravindra Reddy B, Madhavi G (2013a) Application of phytogenic zerovalent iron nanoparticles in the adsorption of hexavalent chromium, Spectrochim. Acta—Part A Mol. Biomol. Spectrosc 116:17–25. https://doi.org/10.1016/j.saa.2013a.06.045

Madhavi V, Prasad TNVKV, Reddy AVB et al (2013b) Application of phytogenic zerovalent iron nanoparticles in the adsorption of hexavalent chromium. Spectrochim Acta—Part A Mol Biomol Spectrosc 116:17–25. https://doi.org/10.1016/j.saa.2013b.06.045

Mali SC, Dhaka A, Githala CK, Trivedi R (2020) Green synthesis of copper nanoparticles using Celastrus paniculatus Willd. leaf extract and their photocatalytic and antifungal properties. Biotechnol Reports 27:e00518. https://doi.org/10.1016/j.btre.2020.e00518

Manjari G, Saran S, Radhakrishanan S et al (2020) Facile green synthesis of Ag–Cu decorated ZnO nanocomposite for effective removal of toxic organic compounds and an efficient detection of nitrite ions. J Environ Manage 262:110282. https://doi.org/10.1016/j.jenvman.2020.110282

Marimuthu S, Antonisamy AJ, Malayandi S et al (2020) Silver nanoparticles in dye effluent treatment: a review on synthesis, treatment methods, mechanisms, photocatalytic degradation, toxic effects and mitigation of toxicity. J Photochem Photobiol B Biol 205:111823. https://doi.org/10.1016/j.jphotobiol.2020.111823

Mohamed EA (2020) Green synthesis of copper & copper oxide nanoparticles using the extract of seedless dates. Heliyon 6:e03123. https://doi.org/10.1016/j.heliyon.2019.e03123

Nabi G, Raza W, Tahir MB (2020a) Green synthesis of TiO_2 nanoparticle using cinnamon powder extract and the study of optical properties. J Inorg Organomet Polym Mater 30:1425–1429. https://doi.org/10.1007/s10904-019-01248-3

Nabi G, Ain QU, Tahir MB, Nadeem Riaz K, Iqbal T, Rafique M, Hussain S, Raza W, Aslam I, Rizwan M (2020b) Green synthesis of TiO_2 nanoparticles using lemon peel extract: their optical

and photocatalytic properties. Int J Environ Anal Chem, 1–9. https://doi.org/10.1080/03067319.2020b.1722816
Nadeem M, Khan R, Afridi K et al (2020) Green synthesis of cerium oxide nanoparticles (Ceo2 nps) and their antimicrobial applications: a review. Int J Nanomedicine 15:5951–5961
Naik GK, Mishra PM, Parida K (2013) Green synthesis of Au/TiO_2 for effective dye degradation in aqueous system. Chem Eng J 229:492–497. https://doi.org/10.1016/j.cej.2013.06.053
Nakata K, Fujishima A (2012) TiO_2 photocatalysis: design and applications. J Photochem Photobiol C Photochem Rev 13:169–189. https://doi.org/10.1016/j.jphotochemrev.2012.06.001
Nanoparticles M (2020) Heterogeneous fenton-like catalytic degradation of
Nguyen NHA, Padil VVT, Slaveykova VI, Černík M, Ševců A (2018) Green synthesis of metal and metal oxide nanoparticles and their effect on the unicellular alga Chlamydomonas reinhardtii. Nanoscale Res Lett 13. https://doi.org/10.1186/s11671-018-2575-5
Pan Z, Lin Y, Sarkar B et al (2019) Green synthesis of iron nanoparticles using red peanut skin extract: synthesis mechanism, characterization and effect of conditions on chromium removal. J Colloid Interface Sci 558:106–114. https://doi.org/10.1016/j.jcis.2019.09.106
Panchal P, Meena P, Nehra SP (2021) A rapid green synthesis of Ag/AgCl-NC photocatalyst for environmental applications. Environ Sci Pollut Res 28:3972–3982. https://doi.org/10.1007/s11356-020-11834-5
Parimala L, Santhanalakshmi J (2014) Studies on the iron nanoparticles catalyzed reduction of substituted aromatic ketones to alcohols. J Nanoparticles 2014:1–10. https://doi.org/10.1155/2014/156868
Pasinszki T, Krebsz M (2020) Synthesis and application of zero-valent iron nanoparticles in water treatment, environmental remediation, catalysis, and their biological effects. Nanomaterials 10. https://doi.org/10.3390/nano10050917
Poguberović SS, Krčmar DM, Maletić SP, Kónya Z, Pilipović DDT, Kerkez DV, Rončević SD (2016) Removal of As(III) and Cr(VI) from aqueous solutions using "green" zero-valent iron nanoparticles produced by oak, mulberry and cherry leaf extracts. Ecol Eng 90:42–49. https://doi.org/10.1016/j.ecoleng.2016.01.083
Prashanth V, Priyanka K, Remya N (2021) Solar photocatalytic degradation of metformin by TiO_2 synthesized using Calotropis gigantea leaf extract. Water Sci Technol 83:1072–1084. https://doi.org/10.2166/wst.2021.040
Pushpamalini T, Keerthana M, Sangavi R, Nagaraj A, Kamaraj P (2020) Comparative analysis of green synthesis of TiO_2 nanoparticles using four different leaf extract. Mater Today Proc 40:S180–S184. https://doi.org/10.1016/j.matpr.2020.08.438
Rafique M, Sadaf I, Tahir MB et al (2019) Novel and facile synthesis of silver nanoparticles using Albizia procera leaf extract for dye degradation and antibacterial applications. Mater Sci Eng C 99:1313–1324. https://doi.org/10.1016/j.msec.2019.02.059
Rai MS, Bhat PR, Prajna PS, Jayadev K, Rao PSV (2014) Original research article degradation of malachite green and congo red using aloe barabadensis mill. Extract 3:330–340
Raman CD, Sellappa K, Mkandawire M (2021) Facile one step green synthesis of iron nanoparticles using grape leaves extract: textile dye decolorization and wastewater treatment. Water Sci Technol 83. https://doi.org/10.2166/wst.2021.140
Ramzan M, Obodo RM, Mukhtar S, Ilyas SZ, Aziz F, Thovhogi N (2021) Green synthesis of copper oxide nanoparticles using Cedrus deodara aqueous extract for antibacterial activity. Mater Today Proc 36:576–581. https://doi.org/10.1016/j.matpr.2020.05.472
Ravikumar KVG, Sudakaran SV, Ravichandran K, Pulimi M, Natarajan C, Mukherjee A (2019) Green synthesis of NiFe nano particles using Punica granatum peel extract for tetracycline removal. J Clean Prod 210:767–776. https://doi.org/10.1016/j.jclepro.2018.11.108
Reddy NV, Li H, Hou T, Bethu MS, Ren Z, Zhang Z (2021) Phytosynthesis of silver nanoparticles using perilla frutescens leaf extract: characterization and evaluation of antibacterial, antioxidant, and anticancer activities. Int J Nanomedicine 16:15–29. https://doi.org/10.2147/IJN.S265003
Rosenberg E (2015) Heavy metals in water: presence, removal and safety. Johnson Matthey Technol Rev 59:293–297. https://doi.org/10.1595/205651315x689009

Roy K, Sarkar CK, Ghosh CK (2015) Rapid colorimetric detection of Hg2+ ion by green silver nanoparticles synthesized using Dahlia pinnata leaf extract. Green Process Synth 4:455–461. https://doi.org/10.1515/gps-2015-0052

Sachan D, Ramesh A, Das G (2021) Green synthesis of silica nanoparticles from leaf biomass and its application to remove heavy metals from synthetic wastewater: a comparative analysis. Environ Nanotechnol Monit Manag 16:100467. https://doi.org/10.1016/j.enmm.2021.100467

Samrot AV, Angalene JLA, Roshini SM, Raji P, Stefi SM, Preethi R, Selvarani AJ, Madankumar A (2019) Bioactivity and heavy metal removal using plant gum mediated green synthesized silver nanoparticles. J Clust Sci 30:1599–1610. https://doi.org/10.1007/s10876-019-01602-y

Sankar R, Rizwana K, Shivashangari KS, Ravikumar V (2015) Ultra-rapid photocatalytic activity of Azadirachta indica engineered colloidal titanium dioxide nanoparticles. Appl Nanosci 5:731–736. https://doi.org/10.1007/s13204-014-0369-3

Sankar R, Manikandan P, Malarvizhi V, Fathima T, Shivashangari KS, Ravikumar V (2014) Green synthesis of colloidal copper oxide nanoparticles using Carica papaya and its application in photocatalytic dye degradation. Spectrochim. Acta—Part A Mol Biomol Spectrosc 121:746–750. https://doi.org/10.1016/j.saa.2013.12.020

Sarma GK, Sen Gupta S, Bhattacharyya KG (2019) Nanomaterials as versatile adsorbents for heavy metal ions in water: a review. Environ Sci Pollut Res 26:6245–6278

Sathishkumar M, Sneha K, Won SW, Cho CW, Kim S, Yun YS (2009) Cinnamon zeylanicum bark extract and powder mediated green synthesis of nano-crystalline silver particles and its bactericidal activity. Colloids Surfaces B Biointerfaces 73:332–338. https://doi.org/10.1016/j.colsurfb.2009.06.005

Sethy NK, Arif Z, Mishra PK, Kumar P (2020) Green synthesis of TiO_2 nanoparticles from Syzygium cumini extract for photo-catalytic removal of lead (Pb) in explosive industrial wastewater. Green Process Synth 9:171–181. https://doi.org/10.1515/gps-2020-0018

Shad S, Belinga-Desaunay-Nault MFA, Sohail, Bashir N, Lynch I (2020) Removal of contaminants from canal water using microwave synthesized zero valent iron nanoparticles. Environ Sci Water Res Technol 6:3057–3065. https://doi.org/10.1039/d0ew00157k

Shaik AM, David Raju M, Rama Sekhara Reddy D (2020b) Green synthesis of zinc oxide nanoparticles using aqueous root extract of Sphagneticola trilobata Lin and investigate its role in toxic metal removal, sowing germination and fostering of plant growth. Inorg Nano-Metal Chem 50:569–579. https://doi.org/10.1080/24701556.2020.1722694

Shaik AM, David Raju M, Rama Sekhara Reddy D (2020a) Green synthesis of zinc oxide nanoparticles using aqueous root extract of Sphagneticola trilobata Lin and investigate its role in toxic metal removal, sowing germination and fostering of plant growth. Inorg. Nano-Metal Chem 50:569–579. https://doi.org/10.1080/24701556.2020a.1722694

Sharma P, Pant S, Dave V, Tak K, Sadhu V, Reddy KR (2019) Green synthesis and characterization of copper nanoparticles by Tinospora cardifolia to produce nature-friendly copper nano-coated fabric and their antimicrobial evaluation. J Microbiol Methods 160:107–116. https://doi.org/10.1016/j.mimet.2019.03.007

Siddiqui VU, Ansari A, Chauhan R, Siddiqi WA (2020) Green synthesis of copper oxide (CuO) nanoparticles by Punica granatum peel extract. Mater Today Proc. https://doi.org/10.1016/j.matpr.2020.05.504

Singh J, Kumar V, Kim KH, Rawat M (2019) Biogenic synthesis of copper oxide nanoparticles using plant extract and its prodigious potential for photocatalytic degradation of dyes. Environ Res 177:108569. https://doi.org/10.1016/j.envres.2019.108569

Sinha T, Ahmaruzzaman M (2015) Green synthesis of copper nanoparticles for the efficient removal (degradation) of dye from aqueous phase. Environ Sci Pollut Res 22:20092–20100. https://doi.org/10.1007/s11356-015-5223-y

Srivastava V, Choubey AK (2021) Study of adsorption of anionic dyes over biofabricated crystalline α-MnO_2 nanoparticles. Environ Sci Pollut Res 28:15504–15518. https://doi.org/10.1007/s11356-020-11622-1

Suresh D, Nethravathi PC, Udayabhanu, Rajanaika H, Nagabhushana H, Sharma SC (2015) Green synthesis of multifunctional zinc oxide (ZnO) nanoparticles using Cassia fistula plant extract and their photodegradative, antioxidant and antibacterial activities. Mater Sci Semicond Process 31:446–454. https://doi.org/10.1016/j.mssp.2014.12.023

Tagad C, Seo HH, Tongaonkar R, Yu YW, Lee JH, Dingre M, Kulkarni A, Fouad H, Ansari SA, Moh SH (2017) Green synthesis of silver nanoparticles using Panax ginseng root extract for the detection of Hg2+. Sensors Mater 29:205–215. https://doi.org/10.18494/SAM.2017.1475

Taj MB, Alkahtani MDF, Raheel A, Shabbir S, Fatima R, Aroob S, Yahya R, Alelwani W, Alahmadi N, Abualnaja M, Noor S, Ahmad RH, Alshater H (2021) Bioconjugate synthesis, phytochemical analysis, and optical activity of NiFe2O4 nanoparticles for the removal of ciprofloxacin and Congo red from water. Sci Rep 11. https://doi.org/10.1038/s41598-021-84983-3

Tan YN, Lee JY, Wang DIC (2010) Uncovering the design rules for peptide synthesis of metal nanoparticles. J Am Chem Soc 132:5677–5686. https://doi.org/10.1021/ja907454f

Tănase MA, Marinescu M, Oancea P, Răducan A, Mihaescu CI, Alexandrescu E, Nistor CL, Jinga L-I, Diţu LM, Petcu C, Cinteza LO (2021) Antibacterial and photocatalytic properties of ZnO nanoparticles obtained from chemical versus Saponaria officinalis extract-mediated synthesis. Molecules 26:2072. https://doi.org/10.3390/molecules26072072

Taşar Ş, Kaya F, Özer A (2014) Biosorption of lead(II) ions from aqueous solution by peanut shells: equilibrium, thermodynamic and kinetic studies. J Environ Chem Eng 2:1018–1026. https://doi.org/10.1016/j.jece.2014.03.015

Turakhia B, Turakhia P, Shah S (2018) Green synthesis of zero valent iron nanoparticles from Spinacia oleracea (spinach) and its application in waste water treatment, Iaetsd J Adv Res. Appl Sci 5:46–51

Vanaja M, Paulkumar K, Baburaja M, Rajeshkumar S, Gnanajobitha G, Malarkodi C, Sivakavinesan M, Annadurai G (2014) Degradation of methylene blue using biologically synthesized silver nanoparticles. Bioinorg Chem Appl 2014. https://doi.org/10.1155/2014/742346

Veisi H, Karmakar B, Tamoradi T, Hemmati S, Hekmati M, Hamelian M (2021) Biosynthesis of CuO nanoparticles using aqueous extract of herbal tea (Stachys Lavandulifolia) flowers and evaluation of its catalytic activity. Sci Rep 11. https://doi.org/10.1038/s41598-021-81320-6

Vinayagam R, Selvaraj R, Arivalagan P, Varadavenkatesan T (2020) Synthesis, characterization and photocatalytic dye degradation capability of Calliandra haematocephala-mediated zinc oxide nanoflowers. J Photochem Photobiol B Biol 203:111760. https://doi.org/10.1016/j.jphotobiol.2019.111760

Wang T, Jin X, Chen Z, Megharaj M, Naidu R (2014) Green synthesis of Fe nanoparticles using eucalyptus leaf extracts for treatment of eutrophic wastewater. Sci Total Environ 466–467:210–213. https://doi.org/10.1016/j.scitotenv.2013.07.022

Weng X, Jin X, Lin J, Naidu R, Chen Z (2016a) Removal of mixed contaminants Cr(VI) and Cu(II) by green synthesized iron based nanoparticles. Ecol Eng 97:32–39. https://doi.org/10.1016/j.ecoleng.2016.08.003

Weng X, Jin X, Lin J et al (2016b) Removal of mixed contaminants Cr(VI) and Cu(II) by green synthesized iron based nanoparticles. Ecol Eng 97:32–39. https://doi.org/10.1016/j.ecoleng.2016.08.003

Wu Z, Su X, Lin X, Khan NI, Owens G, Chen Z (2021) Removal of As(V) by iron-based nanoparticles synthesized via the complexation of biomolecules in green tea extracts and an iron salt. Sci Total Environ 764. https://doi.org/10.1016/j.scitotenv.2020.142883

Xin Lee K, Shameli K, Miyake M, Kuwano N, Bt Ahmad Khairudin NB, Bt Mohamad SE, Yew YP (2016) Green synthesis of gold nanoparticles using aqueous extract of Garcinia mangostana fruit peels. J Nanomater 2016. https://doi.org/10.1155/2016/8489094

Yadav VK, Fulekar MH (2018b) Biogenic synthesis of maghemite nanoparticles (γ-$Fe2O_3$) using Tridax leaf extract and its application for removal of fly ash heavy metals (Pb, Cd). In: Materials today: proceedings. Elsevier Ltd, pp 20704–20710

Yadav VK, Fulekar MH (2018a) Biogenic synthesis of maghemite nanoparticles (γ-Fe2O3) using Tridax leaf extract and its application for removal of fly ash heavy metals (Pb, Cd). Mater Today Proc 5:20704–20710. https://doi.org/10.1016/j.matpr.2018.06.454

Yusefi M, Shameli K, Yee OS, Teow SY, Hedayatnasab Z, Jahangirian H, Webster TJ, Kuča K (2021) Green synthesis of fe3o4 nanoparticles stabilized by a garcinia mangostana fruit peel extract for hyperthermia and anticancer activities. Int J Nanomedicine 16:2515–2532. https://doi.org/10.2147/IJN.S284134

Zahra Z, Habib Z, Chung S, Badshah MA (2020) Exposure route of TiO_2 nps from industrial applications to wastewater treatment and their impacts on the agro-environment. Nanomaterials 10:1–22. https://doi.org/10.3390/nano10081469

Zhu F, He S, Liu T (2018) Effect of pH, temperature and co-existing anions on the Removal of Cr(VI) in groundwater by green synthesized nZVI/Ni. Ecotoxicol Environ Saf 163:544–550. https://doi.org/10.1016/j.ecoenv.2018.07.082